A Thesis

On

FAULT IDENTIFICATION IN ROLLER BEARING USING VIBRATION SIGNATURE ANALYSIS

Submitted in the partial fulfilment of requirement for

the award of degree

MASTER OF ENGINEERING

In

PRODUCTION AND INDUSTRIAL ENGINEERING

By

Sorav Sharma

Regn. No.-800982027

Under the supervision of

Dr. V. P. Agrawal
Visiting Professor

Dr. P. K . Kankar
Assistant Professor

DEPARTMENT OF MECHANICAL ENGINEERING

THAPAR UNIVERSITY, PATIALA (PUNJAB)

July-2011

Dedicated To My Loving Parents

CERTIFICATE

This is to certify that the work done in this thesis report titled "FAULT IDENTIFICATION IN ROLLER BEARING USING VIBRATION SIGNATURE ANALYSIS " submitted in partial fulfilment of requirement for the award of Master of Engineering degree in Production and Industrial Engineering in the Mechanical Department of Thapar University, Patiala is an authentic record of work carried out by me under the guidance of Dr. V. P. Agrawal, Visiting Professor and Dr. P. K. Kankar, Assistant Professor, Mechanical Engineering Department, Thapar University, Patiala.

The matter embodied in this report has not been submitted in part or full to any other university or institute for the award of any degree.

Sorav Sharma
(SORAV SHARMA)

This is to certify that above declaration made by the student concerned is correct to the best of my knowledge & belief.

Dr. V.P. Agrawal
Visiting Professor
Deptt. of mechanical Engg.
Thapar University, Patiala

05.07.11
Dr. P. K. Kankar
Assistant Professor
Deptt. of mechanical Engg.
Thapar University, Patiala

Countersigned by:

Dr. Ajay Batish
Professor & HOD
Deptt. of Mechanical Engg.
Thapar University, Patiala

Dr. S.K. Mohapatra
Dean,
Acadamic Affairs
Thapar University, Patiala

ACKNOWLEDGEMENT

I am highly grateful to the authorities of Thapar University, Patiala for providing this opportunity to carry out the thesis work.

I express my deep gratitude and respects to my guides ***Dr. V. P. Agrawal and Dr. P.K . Kankar*** *for their keen interest and valuable guidance, strong motivation and constant encouragement during the course of the work. I thank them for their great patience, constructive criticism and myriad useful suggestions apart from invaluable guidance to me.*

I thank our head of department ***Dr. Ajay Batish****, whose excellent leadership and administration made this research project very convenient in term of required stuff and nice working condition. I am extremely thankful to member of distinguished faculty.*

The non-teaching staff ***Mr. Rajender, Mr. Sukhbir, Mr. Satwinder Singh, Mr. Charanjit Singh, Mr. Rajinder,*** *deserve special thanks for their help during the period of this work.*

I am also thankful to other faculty members and all the workshop staff of Mechanical Department, Thapar University, Patiala for their support.

Some friends were never too busy to give me a hand whenever they were needed. No word acknowledge the support I received from ***Rajdeep Singh, Karanpreet Singh, Ramandeep Singh, Ankush Kumar, Dhiman Johns, Yogesh Kumar Singla, Manjot Singh Cheema*** *for their valorous help and co-operation.*

Last but not the least, I would like to thank my ***parents*** *and my* ***sisters*** *for always being there when I needed them most and for their moral support that kept my spirit up during the endeavour.*

Sorav Sharma

ABSTRACT

Rolling element bearings are extensively used in most of the rotating machines to support static/dynamic loads. Their performance is utmost important in power stations, chemical plants, automotive industries, aerospace turbo machinery and process industries that require precise and efficient performance. These bearings can take up both radial and axial loads for most of the applications. They have a great influence on the dynamic behaviour of the rotating machines and act as a source of vibration and noise in these systems. There is a critical need to increase reliability and performance of rolling element bearings to prevent catastrophic failure of the machinery.

The present study, identify the effects of localized defect like spall on amplitude of vibration using RSM. The combination effects of these defects on the taper roller bearings are also focused which is not done in most of the studies. This work attempts to analyze vibration responses of a horizontal rotor supported on taper roller bearings. Experimental study of a rotor bearing system has been carried out to obtain the vibration response due to localized defects such as spall on outer race, inner race and roller. Vibration responses obtained show that the every defect excites the system at its characteristic frequency. Response surface methodology also shows that the severe vibration (Max. peak of vibration excitation) occurs in case of bearing with outer race defect. Also interaction of outer and inner race defect produces severe vibrations. Defect in roller has less effect on amplitude of vibration.

TABLE OF CONTENTS

LIST OF FIGURES

LIST OF TABLES

NOMENCLATURE

BPF = Ball Passage Frequency

$\boldsymbol{D}$ = pitch diameter

$\boldsymbol{d}$ = roller diameter

$\mathbf{d_b}$ = diameter of rolling elements

$\mathbf{d_c}$ = cage pitch diameter

$\boldsymbol{k}$ = constant for Hertzian contact elastic deformation

k =waviness order

N = number of discrete points

$\mathbf{N_b}$ **=** number of balls

$\mathbf{N_r}$ **=** number of roller

p = empirical constant for a particular geometry

q = empirical constant for a particular geometry

RMS= Root mean square

RSM = Response surface method

$\boldsymbol{VC}$ = varying compliance

X = rotational frequency

$\overline{\boldsymbol{x}}$ **=** mean acceleration signal

$\boldsymbol{x_i}$ **=** signal from each sampled point

$\mathbf{x_0}$ = factors on which response variable depend

$\mathbf{y_0}$ = response variable of interest

$\boldsymbol{\alpha}$ = contact angle.

$\boldsymbol{\gamma}$ = determine the threshold level

$\boldsymbol{\varepsilon}$ = noise or error observed in the response

$\boldsymbol{\sigma_o}$ = vibration variance varies with load or shaft of the speed.

$\boldsymbol{\omega_{bpfi}}$ = inner race defect frequency

$\boldsymbol{\omega_{bpfo}}$ = outer race defect frequency

$\boldsymbol{\omega_{bsf}}$ = ball spin frequency

$\boldsymbol{\omega_c}$ = rotational frequency of cage

$\boldsymbol{\omega_{cage}}$ = cage rotational frequency

$\boldsymbol{\omega_e}$ = rotational frequency of outer race

$\boldsymbol{\omega_{ep}}$ = rolling element passage frequency of outer race

$\boldsymbol{\omega_i}$ = rotational frequency of inner race

$\boldsymbol{\omega_{ip}}$ = rolling element passage frequency of inner race

$\boldsymbol{\omega_r}$ = rotational frequency of roller

$\boldsymbol{\omega_{rp}}$ = rolling element passage frequency of roller

$\boldsymbol{\omega_{wp}}$ = wave passage frequency

CHAPTER 1

INTRODUCTION

1.1 BACKGROUND

Now a days, maintenance cost is one of the major operating costs in manufacturing companies. Maintenance cost involves spare parts inventory and manpower costs. Unexpected breakdowns, replacement and repair expenses from catastrophic failures indulge in loss of output due to machinery downtime. Adoption of predictive and preventive maintenance procedures, significantly reduces losses from these causes and also improve the maintenance management and perhaps increase the product quality and cost. Predictive maintenance is based on continuous measurement of some machine operating parts, like temperature, power consumption, vibration, noise and forces are commonly employed for this purpose.

Roller element bearings are one of the major machinery components used in industries like power plants, chemical plants and automotive industries that require precise and efficient performance. Applications of rolling element bearings are found in equipment as diverse as paper mill rollers to the space shuttle main engine turbo machinery. Rolling element bearings include all types of bearings that make use of the rolling action of balls or rollers to permit minimum friction, from the constrained motion of one body relative to another (Harris and Kotzalas, 2006). Rolling element bearings are used to permit the rotation of a shaft relative to some fixed structure. However, in some cases these bearings permit translation, that is, relative linear motion, and a few rolling bearing designs permit a combination of relative linear and rotary motions between two bodies. Significant cost saving and profitability can be achieved by equipment availability, reliability and maintainability.

High production volume system, which consist of several automatic and interconnected machine tools, the working environment is very difficult. The human approach for measurement and inspection during the running operation (running machine) is generally tedious and measuring equipment has to be very robust. The large production cost on large transfer line (in high production volume) can be as high as Rs 920000 per hour. The average downtime is in excess of 25 percent, with unexpected bearing failure and tool breakages, as the main causes (Lai, 1990). A predictive maintenance system is capable of only partial reduction of these stoppages, and thus increases the manufacturing productivity.

The machine conditioning and monitoring system also provide the smooth running of roller element bearings, which is vital for the proper functioning of the machine. To avoid sudden failure, it is important to monitor the condition of the bearings. Several techniques are currently available for detection of defect in roller bearing elements. These include vibration and acoustics measurements like overall level, kurtosis, spectral analysis, high frequency resonance, shock pulse, sound pressure and sound intensity and spectrographic oil analysis (oil monitoring). Vibration and acoustics measurement system are quite effective for detecting the defect in roller bearing elements. One approach to study the detection of the defect in roller bearings through measurements, when comparing the response with healthy bearings with that of defective bearings (seeded defects on bearing elements).

1.2 ANALYSIS IN CONDITION MONITORING

Condition Based Monitoring (CBM) is an effective form of predictive maintenance where the condition of specific areas of plant and equipment, can be estimated and monitor. CBM also be done, automatically with the use of instrumentation such as machinery vibration analysis and thermal imaging equipment or manually. In automatic CBM when any monitored and predefined condition limit is exceeded, a signal or output is turned on. Output of the signal is sent directly to a Computerized Maintenance Management System (CMMS) so that a work order is generated automatically. This is particularly suited to continuous process plants where plant failure and downtime are extremely costly like in case of turbines. Machine condition monitoring can be applied to many conditions. Condition monitoring of temperature**,** analysis of machine vibration**,** over voltage or current and liquid level are the most common.

Vibration analysi**s** is the most commonly used technology used to monitor the condition of the machine. The frequency of the vibrations can also be mapped or represented, when certain frequencies will be present. The conditions then indicates about the impending defect of that system. Comparison of the vibration spectra of new equipment versus equipment that has been used, will provide the information and make a decision, whether the maintenance is required or not. Condition Monitoring using IR thermography provides a quick and safe way of detecting problems in many different situations. Modern infrared cameras can be used to detect, increases in temperature that indicate potential problems. These may include increases the temperature of electrical contacts or insulation. Being non-contact**,** infrared thermography

provides a condition monitoring technique that can be often be safely carried out while equipment is running.

CBM is a maintenance program that recommends maintenance actions based on the information collected through condition monitoring. CBM attempts to avoid unnecessary maintenance tasks by taking maintenance actions only when there is evidence of abnormal behaviours of a physical asset. A CBM program, if properly established and effectively implemented, can significantly reduce maintenance cost by reducing the number of unnecessary scheduled preventive maintenance operations.

A CBM program consists of three key steps:

1. *Data acquisition* (information collecting), to obtain data relevant to system health.
2. *Data processing* (information handling), to handle and analyse the data or signals collected from the data acquisition for better understanding and interpretation of the data.
3. *Maintenance decision-making* (decision-making), to recommend efficient maintenance policies.

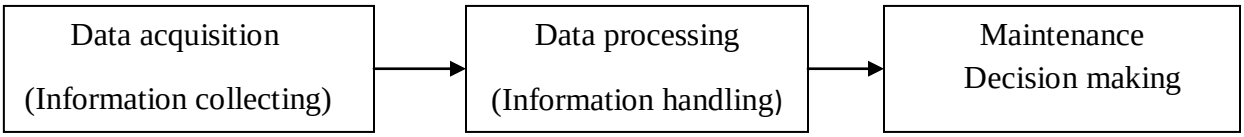

Figure 1.1: Steps of CBM

1.2.1 Aspects in A CBM Program

There are two aspects in CBM program

1. Diagnostics
2. Prognostics

Diagnostics deals with fault detection, isolation and identification when it occurs. Fault detection is a task to indicate whether something is going wrong in the monitored system; fault isolation is a task to locate the component that is faulty; and fault identification is a task to determine the nature of the fault when it is detected.

Prognostics deals with fault prediction before it occur. Fault prediction is a task to determine whether a fault is impending and estimate how soon and how likely a fault will occur. Diagnostics is posterior (later) event analysis and a prognostic is prior event analysis. A

prognostic is much more efficient than diagnostics to achieve zero-downtime performance (Jardine et al., 2005). Diagnostics however, is required when fault prediction of prognostics fails and a fault occurs. A CBM program can be used to do diagnostics or prognostics, or both.

1.3 VIBRATION BASED CONDITION MONITORING ON BEARINGS

Vibration has been used to determine the mechanical condition of machinery and their parts since last 50 years. Many researchers have tried different approaches and different descriptors under different environment and tried to investigate the relationship between the tested bearing and changes in vibration response under operating condition. Displacement, velocity, acceleration, peak acceleration, RMS of overall acceleration, crest factor, frequency spectrum analysis, spike energy, shock pulse, acoustics emission, cepstrum and statistical descriptors such as mean, standard deviation, skew and kurtosis have been reported as useful in evaluating the bearing condition.

1.3.1 Vibration Measurement Techniques

Vibration signal processing techniques and signal metrics commonly used to detect bearing defects**.** Condition monitoring using vibration measurement can be classified into time domain technique, frequency domain technique and time-frequency technique.

1.3.1.1 Time domain technique

Signal analysis in the time domain has been used to monitor the machine conditions. However, complex signals are difficult to analyze, when frequently encountered in industrial equipment. Some of the time domain techniques can be used or applied for condition monitoring, such as root mean square (RMS), mean, peak value, crest factor, kurtosis, and shock pulse counting.

Root mean square

Root mean square (RMS), measures the overall level of a discrete signal.

$$\text{RMS(x)} = \sqrt{\frac{{x_i}^2}{N}}$$

where N is the number of discrete points and x_i represents the signal from each sampled point. The RMS is a powerful tool to estimate the average power in system vibrations. A substantial amount of research has employed RMS to successfully identify bearing defects using accelerometer and AE sensors.

Mean

The mean acceleration signal is the standard statistical mean value. Unlike RMS, the mean is reported only for rectified signals since for raw time signals, the mean remains close to zero. As the mean increases, the condition of the bearing appears to deteriorate.

$$\bar{x} = \frac{1}{N} * \sum_{i=1}^{N} x_i$$

Peak value

Peak value is measured in the time domain or frequency domain. Peak value is the maximum acceleration in the signal amplitude.

Crest factor

Crest factor is the ratio of peak acceleration over RMS. This metric detects acceleration bursts even if signal RMS has not changed. However, crest factor can be counterintuitive. At advance stages of material wear, bearing damage propagates, RMS increases, and crest factor decreases. But crest factor is unreliable to locate defects in rolling elements.

$$\text{Crest Factor} = \frac{\text{Peak acceleration}}{RMS\,(x)}$$

Statistical moments

Machined or ground surfaces in bearings show a random distribution of asperities that are commonly described with the normal distribution function. For this reason, various statistical moments can describe the shape of distribution curves therefore, assessing bearing surface damage level. Equation defines the third moment or skewness as

$$\text{Skewness} = \frac{1}{N-1} \sum_{i=1}^{N} (x_i - \bar{x})^3$$

where *x* is the mean value. For normally distributed data sets the odd moments are zero, unless the time domain signal is rectified. Hence, skew can easily track for bearing conditions.

The normalized fourth moment, kurtosis, is the ratio of the fourth moment to the square of the second moment (commonly known as variance). A good surface finish has a theoretical kurtosis of 3, and when kurtosis increases the surface finish deteriorates, The skew and kurtosis are insensitive to loads and speeds (Kurfess et al., 2006). However, the level of noise between individual readings hampered the detection of bearing damage.

$$\text{Kurtosis} = \frac{(N-1)\sum_{i=1}^{N}(x_i - \bar{x})^4}{\sum_{i=1}^{N}(x_i - \bar{x})^2}$$

Shock pulse counting

Shock pulse counting records the number of pulses larger than a threshold value. This approach works because bearing defects generate, sharply rising impulses with amplitudes larger than noise. However, this technique does not localize the damage of the defect.

1.3.1.2 Frequency domain techniques

Another conventional approach is processing the vibration signals in the frequency domain. The basic indicator is the characteristic defect frequencies in the frequency domain analysis. The characteristic defect frequencies depend on the rotational speed and the location of the defect in a bearing. The presence of the defect frequencies in the direct or processed frequency spectrum is the powerful sign of the fault. The signature of the defected bearing is spread across a wide frequency band and can be easily masked with low frequency machinery vibrations and noise. The consecutive impact between the defect and rolling elements excites the resonances of the structure and the resonant frequencies dominate the frequency spectrum. Therefore, the characteristic defect frequencies cannot be easily noticed because of their low amplitudes with respect to resonant amplitudes.

Frequency domain or spectrum analysis is applied most often to monitor machine condition. However, a simple Fourier transformation at low frequency has limitations in bearing defect detection. Researchers have developed signal processing techniques to enhance defect frequencies over mechanical noise. There are three standard techniques used for monitoring the machine condition (Kurfess et al., 2006). The signal average method, cepstrum analysis, and high-frequency resonance technique.

Signal average

Signal averaging improves statistical accuracy, but it does not improve signal-to noise ratio. Signal average is used to develop an average scheme. When the vibration signature is a generalized periodic functions, then spectrum analysis detects peaks at its characteristic defect frequencies.

Cepstrum analysis

This technique groups patterns of sidebands and harmonics from the spectrum into one signature. Cepstrum detects periodicities in the spectrum while being insensitive to transmission path. The technique works well if the defect frequency signal has not been convoluted with other signals.

High-frequency resonance technique (HFRT)

The high-frequency resonance technique, also known as demodulated resonance analysis or envelope power spectrum, exploits the large amplitude of defect signals around a resonance. HFRT, while being highly sensitive to initial bearing damage, provides an enveloped signal with a high signal-to-noise ratio free of mechanical noise. The following steps, are obtain this envelope signal.

(a) Band pass filtering around the system resonant frequency: The signal in is band passed around a system resonant frequency resulting. The center frequency coincides with the largest amplitude resonant frequency.

(b) Non-linear rectification of the band passed signal: A non-linear rectifier demodulates the band passed signal resulting in the signal.

(c) Cancel high frequency components with a low pass filter: The output signal of the low pass filter, is denoted enveloped signal and will have nonzero values at the harmonics of the deterministic defect frequencies. The HFRT is a powerful and widely used tool that separates defect frequencies from vibrations generated by other mechanical elements. Multiple bearing damages or severely damaged bearings may partially cancel various components in the envelope spectrum. In practice, broadband noise corrupts the envelope signal of a damaged bearing. Hence, the Adaptive Line Enhancer (ALE) can further enhance this signal.

Fast fourier transformation (FFT)

FFT converts the convolution in one domain into a multiplication in the other domain. FFT simplify the solution of many problems, but it is also useful in graphical illustrations of many relationships. Convolution is the operation by which the output (response) of a linear system is obtained from the input (forcing function) and the transfer properties of the physical system, in the time domain represented by its impulse response function. The impulse response function (IRF) of a system is its output when excited by a unit impulse at time zero. FFT shows the

graphical representation of the data and interpretate the data, frequency v/s Amplitude and many more.

1.3.1.3 Time-frequency analysis

Vibration signals measured from machine can be broadly categorized as stationary and non-stationary signals. Stationary signals are the signals, whose statistics do not change with time. In other words, these signals are having time independent statistical properties such as mean value or auto-correlation function. In contrast, non-stationary signals are the signals, whose statistical properties change with time such as vibration during the start-up of an engine. Frequency domain methods are suitable for stationary signals. While, non-stationary or transient signals can be analyzed by applying time-frequency domain techniques such as the short-time Fourier transform (STFT), the Wigner-Ville distribution, and the wavelet transform (WT).

The Wavelet Transform (WT) provides a time-frequency map of the signal being analyzed. The improvement that the WT makes over the STFT is that it can achieve high frequency resolutions with sharper time resolutions. Wavelet is defined as a waveform of effectively limited duration that has an average value of zero. Wavelet analysis is a windowing technique with variable-sized regions. It allows the use of long time intervals for more precise low-frequency information, and shorter regions for high-frequency information. Unlike the Fourier analysis in which a signal is decomposed into its harmonics using global sinusoidal functions that go on forever, in wavelet analysis the signal is broken down into a series of local basis functions called wavelets. Each wavelet is located at a different position on the time axis and is local in the sense that it decays to zero when sufficiently far from its center. At the finest scale, wavelets may be very short indeed; at a coarse scale, they may be very long. Any particular local feature of a signal can be identified from the scale and position of the wavelets into which it is decomposed. Wavelet analysis can often compress or de-noise a signal without appreciable degradation.

1.4 TYPES OF DEFECT IN BEARINGS

Bearing defects may be categorized into two parts:

(a) Localized defects

(b) Distributed defects

(a) Localized defects: Localized defects include cracks, pits and spalls on the rolling surfaces. The mode of failure of rolling element bearings is spalling of the races or the rolling elements, caused when a fatigue crack begins below the surface of the metal and propagates towards the surface until a piece of metal breaks away to leave a small pit or spall. Fatigue failure may be due to overloading or shock loading of the bearings during running and installation. Pitting or cracks occurs due to excessive shock loading .Whenever a local defect on an element interacts with its mating element, sharp changes in the contact stresses at the interface and generates a pulse of very short duration. This pulse produces vibration and noise which can be monitored to detect the presence of a defect in the bearing. Localized defects are shown in Figure 1.2.

(a) Inner Race with Spall **(b)** Outer Race with spall **(c)** Roller with spall

Figure1.2 Spall in inner race(a), outer race(b) and on roller(c)

(b) Distributed defects: Distributed defects include surface roughness, waviness, misaligned races and off-size rolling elements. If the surface feature of the wavelength of the bearing is lesser than the hertzian contact width of the rolling element raceway contact, then it is known as Roughness. If the feature of the wavelength of the bearing is longer than the Hertzian contact width of the rolling element raceway contact, then is known as Waviness, shown in Figure 1.3(a). Distributed defects are caused by manufacturing error, improper installation or abrasive wear. The variation in contact force between rolling elements and raceways due to distributed defects results in an increased vibration level. Some of the distributed defects are shown is Figure 1.3.

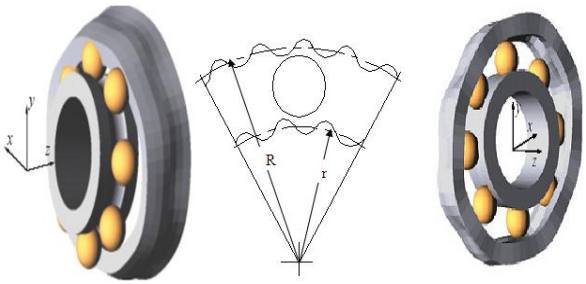

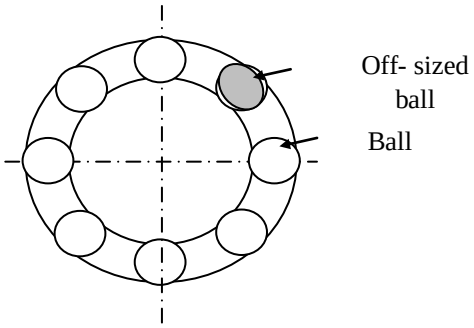

Figure 1.3(a) Waviness at inner and outer race **Figure 1.3 (b) Off-sized ball**

Figure 1.3 Distributed defects (Kankar, 2011)

1.5 BEARING FAILURE MODES

The normal service life of a rolling element bearing rotating under load is determined by material fatigue and wear at the running surfaces. Premature bearing failures can be caused by a large number of factors, the mos**t** common of which are fatigue, wear, plastic deformation, corrosion, brineiling, poor lubrication, faulty installation and incorrect design (Chen, 2000)**.** Common modes of bearing failure are discuss below:

(a) Fatigue

A bearing subject to alternating normal loads could fail due to material fatigue after a certain operation time. Fatigue damage begins with the formation of minute cracks below the bearing surface. As loading continues, the cracks progress to the surface where they cause material to break loose in the contact areas**.** The actual failure can manifest itself as pitting, spalling or flaking of the bearing races or rolling elements. If the bearing continues in service, the damage will spread in the locality of the defect is due to stress concentration. The surface damage severely disturbs the nominal motion of the rolling elements by introducing short time impacts repeated at the characteristic rolling element defect frequencies. As the damage continues to spread the repetitive nature of the impacts will diminish as the motion of the rolling element becomes so irregular and disturbed that it is impossible to distinguish between individual impacts. If the bearing were to continue in service, the damage may spread to other raceways or rolling elements and eventually lead to increased friction and temperature followed by complete seizure.

(b) Wear

Wear is another common cause of bearing failure. It is caused mainly by dirt and foreign particles entering the bearing through inadequate sealing or due to contaminated lubricant. The abrasive foreign particles roughen the contacting surfaces giving a dull appearance. Severe wear changes the raceway profile and alters the rolling element profile and diameter, increasing the bearing clearance. The rolling friction increases considerably and can lead to high levels of slip and skidding, the end result of which is complete breakdown.

(c) Plastic deformation

Plastic deformation of bearing contacting surfaces can be the result of a bearing subject to excessive loading while stationary or undergoing small movements. The result is indentation of the raceway as the excessive loading causes localized plastic deformation. In operation, the deformed bearing would rotate very unevenly producing excessive vibration and would not be fit for further service.

(d) Corrosion

Corrosion damage occurs when water, acids or other contaminants in the oil enter the bearing arrangement. This can be caused by damaged seals, acidic lubricants or condensation which occurs when bearings are suddenly cooled from a higher operating temperature in very humid air. The result is rust on the running surfaces which produces uneven and noisy operation as the rust particles interfere with the lubrication and smooth rolling action of the rolling elements. The rust particles also have an abrasive effect and generate wear. The rust pits also form the initiation sites for subsequent flaking and spalling.

(e) Brinelling

Brinelling manifests itself as regularly spaced indentations distributed over the entire raceway circumference, corresponding approximately in shape to the Hertzian contact area. Three possible causes of brinelling are (1) static overloading which leads to plastic deformation of the raceways, (2) when a stationary rolling bearing is subject to vibration and shock loads and (3) when a bearing forms the loop for the passage of electric current. In all cases, the result will be repetitive indentations of the raceways. In some instances, a large number of indentations may occur as the bearing may occasionally be turned slightly. The bearing operation will be noisy and uneven in the presence of brinelling with each indentation acting like a small fatigue site

producing sharp impacts with the passage of the rolling elements. Continued operation will lead to the development of spalling at the indentation sites and increasing distributed damage.

(f) Lubrication

Inadequate lubrication is one of the common causes of premature bearing failure as it leads to skidding, slip, increased friction, heat generation and sticking. At the highly stressed region of Hertzian contact, when there is insufficient lubricant, the contacting surfaces will weld together, only to be torn apart as the rolling element moves on. The three critical points of bearing lubrication occur at the cage-roller interface, the roller-race interface and the cage-race interface. Lubricant starvation or improper lubricant selection can have severe consequences as the increased temperature can anneal the bearing elements reducing hardness and fatigue life as well as degrading the lubricant. Excessive wear of the bearing elements results, followed by catastrophic failure.

(g) Faulty installation

Faulty installation can include such effects as excessive preloading in either radial or axial directions, misalignment, loose fits or damage due to excessive force used in mounting the bearing components. Radial preloading results in noisier running and usually also in increased temperature differences between the inner and outer races. The increased temperature differences are likely to increase the undesirable preloads, causing higher contact pressures leading to premature fatigue, heavy rolling element wear, overheating and eventual seizure. Oval preloading can result from out-of-round shafts or housings, causing deformation of the inner or outer raceways leading to additional radial preloading. A preload can also be generated by misalignment of the inner and outer races relative to one another causing the rolling elements to run under preload in the apex zones. Such misalignment generates a uniformly wide wear track at the rotating raceway extending over the entire circumference. At the stationary raceway, the track will be of uneven width extending diagonally over the raceway. Excessive axial preload originates from too tight an adjustment in the axial direction during installation. Premature fatigue, heavy rolling element wear and overheating will be the end result. If improper mounting methods are used in the assembly of the bearing in the rotating machine, indentation or scoring damage of the raceways or rolling elements can be caused. Even if the damage is small, it can develop into premature spalling.

(h) Incorrect design

Incorrect design can involve poor choice of bearing type or size for the required operation, or inadequate support by the mating parts. Incorrect bearing selection can result in any number of problems depending on whether it includes low load carrying capability or low speed rating. The end result will be reduced fatigue life and premature failure. Inadequate support can give rise to excessive clearance of the mating parts of the bearing resulting in relative motion such as slippage of the inner race on the shaft. Fretting can occur if the slippage is slight and continuous, generating abrasive metal particles. The looseness will be self perpetuating and will lead to increased friction and temperature resulting in catastrophic failure.

1.6 DESCRIPTION OF TAPER ROLLER BEARING

The inner and outer ring raceways are segments of cones and the rollers are also made with a taper so that the conical surfaces of the raceways and the roller axes if projected, would all meet at a common point on the main axis of the bearing.

This conical geometry is used as it gives a larger contact patch, which permits greater loads to be carried than with spherical (ball) bearings, while the geometry means that the tangential speeds of the surfaces of each of the rollers are the same as their raceways along the whole length of the contact patch and no differential scrubbing occurs. When a roller slides rather than rolls, it can generate wear at the roller-to-race interface, i.e. the differences in surface speeds creates a scrubbing action. Wear will degenerate the close tolerances normally held in the bearing and can lead to other problems. Much closer to pure rolling can be achieved in a tapered roller bearing and this avoids rapid wear.

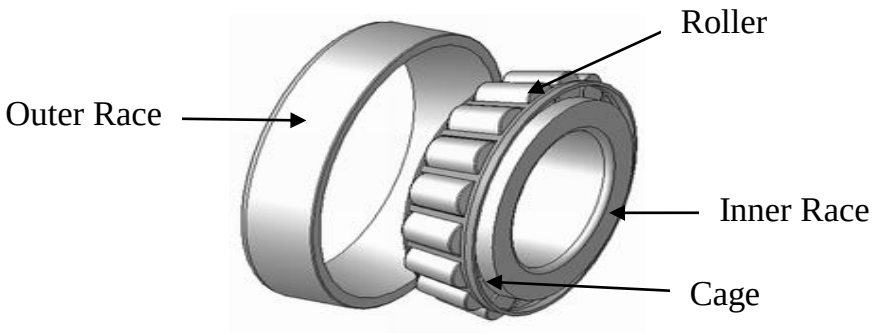

Figure 1.4 Taper roller bearing (Silberwolf, 2006)

The rollers are guided by a flange on the inner ring. This stops the rollers from sliding out at high speed due to their momentum. The larger the half angles of these cones the larger the axial force that the bearing can sustain.

Tapered roller bearings are separable and have the following components: outer ring, inner ring, and roller assembly (containing the rollers and a cage) as shown in Figure 1.4. The non-separable inner ring and roller assembly is called the cone, and the outer ring is called the cup. Internal clearance is established during mounting by the axial position of the cone relative to the cup.

1.6.1 Advantages of Taper Roller Bearing

(a) Radial and axial load: High radial and axial load carrying capacity as compared to ball bearing.

(b) Rigidity: High rigidity and ease of fitting are the essential characteristics of single row tapered roller bearings. If properly fitted it can absorbs impact and shock loads.

(c) Longer rating life: Basic rating life approx. 70 % longer due to improved surfaces, higher performance materials with special heat treatment and optimised contact geometry. For certain applications, this means that a smaller bearing arrangement can be designed.

(d) Lower temperatures: Improved friction behaviour due to optimised surfaces and higher geometrical accuracy.

(e) Reduced noise: Due to improved geometry, optimised surfaces, higher geometrical accuracy.

1.6.2 Applications

Some of the applications of taper roller bearing are given below:

(i) Car and wheel bearing arrangements for road vehicles.

(ii) Agriculture, Construction & Mining Equipment.

(iii) Various Axle Systems.

(iv) Conveyance Vehicles.

(v) Gear Box, Engine Motors, Reducers etc.

In this study, 30304 taper roller bearing has been used. These bearings have applications in various automobile components like front and rear hub and also in heavy duty

trucks, construction machinery and transmission of Yamaha bikes (Model RT180J, RT100K, RT100L and 2000 RT100M).

1.7 ORGANIZATION OF THE THESIS

The thesis is described in five chapters, the details are as follows :

Chapter 1 gives an introduction to a rotor bearing system and condition based monitoring system. Vibration measurement technique and bearing faults and their root causes are also discussed. The objective of the present analysis has also been emphasized along with the organization of the work.

Chapter 2 deals with a review of the published literature. Main focus is on various types of defects in bearing, experimental studies on rotor bearing systems including vibration response and signal processing techniques for fault diagnosis, also on the response surface methodology.

Chapter 3 concerns with problem formulation.

Chapter 4 presents experimentation on the taper roller bearings, also discuss about the experimental setup and later on the dynamic analysis of a horizontal rotor supported on taper roller bearings has been studied with or without defect. FFT technique has been used. RSM procedures are used to conduct several trials for investigating simultaneous effect of defects and rotor speeds

Chapter 5 provides a comprehensive discussion and conclusions arising out of the present work.

CHAPTER 2
LITERATURE REVIEW

A large number of approaches/methodologies for fault diagnosis of rolling element bearings have been reported in the previously published literature. Fault diagnosis is the process of identifying forthcoming or incipient failures in processes or/and systems. In this chapter, previously published research work related to fault diagnosis of rolling element bearings has been reviewed.

Rahnejat and Gohar (1985) have reported the vibrations of radial ball bearings. They studied, squeeze film damping for the rolling motion of a rigid rotor supported on two identical bearings. They showed that even in the presence of an elasto-hydrodynamic lubricating film between the balls and the races, a peak at the Ball Passage Frequency (BPF) appears in the spectrum. As expected, resonance occurs when the BPF coincides with the natural frequency. Envelope detection or the high-frequency resonance technique (HFRT) is an important signal processing technique, which helps in the identification of bearing defects by extracting characteristic defect frequencies (which may not be present in the direct spectrum) from the vibration signal of the defective bearing.

Lim and Singh (1990) have developed a mathematical model for rolling element bearings. A comprehensive bearing stiffness matrix has been proposed by them and it demonstrates a coupling between the shaft bending motion and the flexural motion on the casing plate. Prasad (1991) has investigated on the pitch and width of corrugations on the surfaces of ball bearings. These have been theoretically analyzed, based on kinematics and operating conditions, and found to match closely those of the measured values.

Jun et al. (1995) have investigated the detection and diagnosis of localised defects in rolling element bearings using hypothesis test theory. It is seen that the vibration of damaged bearings consists of two alternating zero-mean Gaussian components, with different Variances, representing background noise and defect signature respectively. They concluded that bearing localised defect detection and diagnosis scheme based on hypothesis test theory, is implemented on a microcomputer and applied to measured vibration signals of normal and faulty bearings, under different thrust loads and at different rotational speeds. The hypothesis

test theory provides a basis for determining the test threshold based on the false alarm probability specified by the user. Researcher believes that a threshold selected to be the average signal energy ($\gamma = N \sigma_o^2$) may also work. However, this false alarm probability, function of vibration variance σ_o that varies with load or shaft speed.

Tandon and Choudhury (1997) have studied the analytical model for the prediction of the vibration response of rolling element bearings due to a localized defect. Analytical model has been proposed for predicting the vibration frequencies of rolling Bearings components and the amplitudes of significant frequency components due to a localized defect on outer race, inner race or on one of the rolling elements under radial and axial loads. The model predicts a discrete spectrum having peaks at the characteristic defect frequencies and their harmonics. In the case of an inner race defect or a rolling element defect under a radial load, there are sidebands around each peak. Experimental was taken on 6002 deep groove ball bearings. The model predicts a frequency spectrum having peaks at characteristic defect frequencies. The amplitudes at these frequencies are also predicted for various defect locations. It is concluded that amplitude for the outer race defect is found quite high as compare to inner race and roller elements defects. Also found that if the amplitude level increases, load also increases. Later on they also studied on the vibration and acoustic measurement methods for the detection of defects in rolling element bearings (Tandon and Choudhury, 1999). In this paper, detection of two categories of defect has been considered, localized and distributed defect. Detection of defects is then measured by vibration and noise generation in bearings. Vibration measurement in both time and frequency domains along with signal processing techniques such as the high-frequency resonance technique have been covered. Acoustic measurement techniques such as sound pressure, sound intensity and acoustic emission have been reviewed. They concluded that Vibration in the time domain can be measured through parameters such as overall RMS level, crest factor, probability density and kurtosis. Among these, kurtosis is the most effective. The shock pulse method has also gained wide industrial acceptance. In acoustic measurement both sound pressure and sound intensity have been used for the detection of the bearing defect. The sound intensity technique seems to be better than sound pressure measurements for bearing diagnostics.

Brändlein et al. (1999) have investigated the defectives frequencies Ball and Roller Bearings. Assuming no slip and considering outer race to be stationary, the general forms of the bearing defect frequency equations are given below:

Inner race defect frequency $$\omega_{bpfi} = \frac{N_b \omega_{inner}\left(1+\frac{d}{D}\cos(\alpha)\right)}{2}$$

Outer race defect frequency $$\omega_{bpfo} = \frac{N_b \omega_{inner}\left(1-\frac{d}{D}\cos(\alpha)\right)}{2}$$

Cage rotational frequency $$\omega_{cage} = \frac{\omega_{inner}\left(1-\frac{d}{D}\cos(\alpha)\right)}{2}$$

Ball or Roller spin frequency $$\omega_{bsf} = \frac{\omega_{inner}}{2}\frac{D}{d}\left(1-\left(\frac{d}{D}\cos(\alpha)\right)^2\right)$$

The bearing frequency equations provide a theoretical estimation of the frequencies to be expected, when various defects occur on the bearing elements. These frequencies are calculated based upon the assumption that an ideal impulse is generated whenever a bearing element encounters the defect.

Bachschmid et al. (2002) have studied a model-based identification method for multiple faults, by means of a model-based identification in the frequency domain. The method requires the definition of models of elements that compose the system, i.e., the rotor, the bearings and the foundation, as well as the models of the faults, which can be represented by harmonic components of equivalent force or moment systems. The models of several types of faults are analyzed in detail.

Harsha et al. (2004) have developed the analytical model to predict non-linear dynamic responses in a rotor bearing system due to surface waviness developed. Surface waviness is developed on outer and inner race. The results are presented in the form FFT. They investigated that outer race waviness occurs, when the number of ball is equals to waves i.e the waviness order for sever vibration is $k = N_b$. The axial vibrations appears at an integer multiple of the BPF $q(N_b \times \omega_{cage})$. In case of the inner race waviness, the transformations of the peaks can be at

$q(\omega_{wp} \pm p\ \omega_{cage})$. Peak amplitude of vibration and super harmonic appear at the wave passage frequency. Hence from this analysis the prediction about the major peaks at frequencies can be made.

Harsha (2005 (a)) has presented the non-linear dynamic response of a balanced rotor supported on rolling element bearings. Analytical formulation of the contacts between the balls and races are considered as non-linear springs, whose stiffness are obtained by using Hertzian elastic contact deformation theory. Parametric study done by taking radial internal clearance and rotor speed has been resulted. The appearance of regions of periodic, sub harmonic and chaotic behaviour is seen to be strongly dependent on the radial internal clearance and rotor speed. Poincare maps and frequency spectra are used to understand the effect of the system. It is concluded that the non-linear response of an balanced rotor with internal radial clearance has been demonstrated to be chaotic for some specific combination of non-linear stiffness and rotational speed combined with a misalignment of races to provide sufficient non-linearity. Later on Harsha (2005(b)) has also analyzed nonlinear dynamic behaviour of an unbalanced rotor supported by roller bearing. The non-linearity in the rotor bearing system is due to Hertzian contact, unbalanced rotor effect and radial internal clearance. The system excite due to varying compliance frequency and the rotational frequency of the shaft. It was investigated that under unbalanced rotor, varying compliance frequency and rotational frequency of the shaft exist together in rolling element frequencies. The theoretical analysis for a rigid horizontal rotor-ball-bearing model with unbalanced force shows that multi frequency excitation due to varying compliance and unbalanced force results in a response, which has regions of instability and chaos. Period doubling results in the appearance of 1X/10 and its multiples. Frequency spectra display multiples of 1X and *VC* and the linear combination of the two frequencies. The ratio of the carrier frequency (*VC*) to the modulating frequency decreases with increasing speed.

Harsha and Kankar (2004) have investigated the Stability analysis of a rotor bearing system due to surface waviness and number of balls. In the analytical formulation, the contacts between balls and races are considered as nonlinear springs, whose stiffness are obtained by using Hertzian elastic contact deformation theory. Newton–Raphson method is used to solve the nonlinear differential equations. The effects of surface waviness and the varying number of

balls on stability of rotor bearing system are observed. All results presented in form of fast fourier transformations. They concluded that:

1. Nonlinear dynamic responses are found to be associated with ball passage frequency. Ball passage frequency is the system characteristics and the prediction about system behavior can be made by BPF to avoid resonance.

2. When the number of balls is increased, the center of oscillations approaches zero implying a stiffer system. From this it can be predicted that increasing the number of balls will reduce the effect of the BPF. However, in the case the BPF coincides with the natural frequency at a relatively low rotor speed since it is the cage speed times the number of balls.

3. The axial vibrations appears at an integer multiple of the ball passage frequency $q(N_b \times \omega_c)$.

The waviness order and vibration frequency for the outer race waviness follows the formula as

Waviness of orders : $k = qN_b \pm p$

Vibration caused by waviness : $q\, N_b\, \omega_c$

It is also shown that the system exhibit dynamic behaviours that are extremely sensitive to small variations of the system parameters, such as number of balls and number of waves.

Kiral and Karagulle (2006) have studied the vibration analysis of rolling element bearings with various defects under the action of an unbalanced force. Single and multiple defects on the different bearing components was made and then defect is detected through time and frequency domain techniques. Time and frequency domain parameters such as RMS, crest factor, kurtosis and band energy ratio for the frequency spectrum of the enveloped signals are used to analyse the effect of the defect location and the number of defects on the time and frequency domain parameters. Condition monitoring of the rolling element bearings, generally the direction of the radial force is assumed to be constant, and the bearing structure is assumed to be excited from the same region defined by the load distribution expression. Defect position on the outer ring, number of defects and defect locations, on the inner ring or on the rolling element, and the shaft speed affect the statistical indices. The envelope method can be used efficiently in order to detect the outer and inner ring defects but rolling element defects are not easy to detect through band energy ratio procedures.

Harsha (2006) has investigated nonlinear dynamic analysis of rolling element bearings due to cage run-out and number of balls. Due to run-out of the cage, the rolling elements no longer stay equally spaced. Cage run-out resulting transition from no contact to contact state between

rolling elements and races. The results are presented in form of FFT (fast Fourier transformations) and phase trajectories. This paper also discussed about BPF (ball pass frequency) which is (N_b x ω_c) or also known as varying compliance frequency. It was investigated that the nonlinear response of a perfectly rigid balanced rotor due to self-excited vibration in a ball bearing with small cage run-out is studied. The self-excited vibrations are due to varying compliance of the bearing, which arises because of the geometric and elastic characteristics of the bearing assembly varying according to cage position. It was also investigated that a single off-sized ball within a bearing produces vibrations at the cage speed. Increasing the number of balls means supporting the rotor therefore increasing the system stiffness and reducing the vibration amplitude. It was predicted that the number of balls will reduce the effect of the BPF and because of the cage run-out, the modulating frequency dominant in the vibration spectrum. Later on Harsha and Nataraj (2008) also studied the effect of bearing cage run-out on the nonlinear dynamics of a rotating shaft. Analytical model is used to investigate the nonlinear dynamic behavior of an unbalanced rotor-bearing system due to cage run-out. Due to run-out of the cage, the rolling elements no longer stay equally spaced. The results are presented in the form of fast Fourier transformations and Poincare maps. The system is bi-periodically excited, one due to cage run-out, which is at ball passage frequency and the other due to the unbalance excitation in the rotor, which is at the rotational frequency. Peak amplitudes of vibrations appearing in the spectrum at the ball passage frequency (BPF). They concluded and predicted that increasing the number of balls will reduce the effect of the modulating frequency and because of the cage run-out, ball passage frequency becomes dominant in the vibration spectrum. Our analysis predicts that the highest vibrations due to cage run-out for a generic number of balls are at ($\omega = q\omega_{bp} \pm k\omega_c$ Hz).

1. For the system considered, this happens when the number of balls is more than 14 and with an unbalanced rotor force of 15% of the radial load. The system responses are not chaotic but quasi-periodic, this happens when the number of balls is more than 8 but less than 13.

2. The responses are unpredictable, being either periodic or chaotic and extremely sensitive to both the initial conditions and small variations in the system parameters, this happens when the number of balls is less than 8.

Purushotham et al. (2005) have presented the Multi-fault diagnosis of rolling bearing elements using wavelet analysis and hidden Markov model based fault recognition. This method is used

for detecting localized bearing defects based on wavelet transform. Wavelet transform is basically time–frequency distribution from which periodic structural ringing due to repetitive force impulses, generated upon the passing of each rolling element over the defect, are detected. This paper also presents the pattern recognition for bearing fault monitoring using hidden Markov Models (HMMs). They concluded that wavelet decompositions of the time signals are used to detect bearing race faults. Since wavelet transform is an emerging technique for fault detection and its aim to be stressed in the fault detection of bearings. This paper also discussed the new approach for bearing monitoring that is HMM. Through the usage of this modal, no assumptions are made with regard to the measured signals. Training the models on processed data helps to ensure validate of the models.

Orhan et al. (2006) have studied the vibration monitoring for defect diagnosis of rolling element bearings as a predictive maintenance tool. In this study, the vibration monitoring and analysis case studies were presented and examined in machineries in real operating conditions. Failures formed on the machineries in the course of time were determined by the spectral analysis. Diagnosing techniques of the ball and cylindrical roller element bearing defects were investigated by vibration monitoring and spectral analysis as a predictive maintenance tool. Ball bearing outer race defect and a cylindrical bearing outer race defect were successfully diagnosed. It was shown that ball and cylindrical roller bearing defects were progressed in identical manner without depending on rolling element type. It was investigated that when a bearing defect reaches an advanced stage, high frequency amplitude levels often decrease due to "*self- peening*" of the bearing flaws. It was concluded that if vibration monitoring is applied within regular selected periods, capable instrumentation and if vibration analysis is performed by experienced personnel, impending failures can be easily detected.

Harsha (2006) has investigated the nonlinear dynamic response of a balanced rotor supported by rolling element bearings due to radial internal clearance effect. The mathematical formulation accounted for tangential motions of rolling elements as well as inner and outer races with sources of nonlinearity such as Hertzian contact force and internal radial clearance resulting transition from no contact to contact state between rolling elements and races. The effect of radial internal clearance for rotor bearing system in which rolling element bearings show periodic, quasi-periodic and chaotic behaviour are analyzed. Time response, rotor trajectories, Poincare` maps and power spectra are used. It was concluded that by Varying the

internal radial clearance bound the region of quasi-periodic, sub-harmonic and chaotic for ball bearing excited by various defects. Decrease in radial clearance increase the linear characteristics of the system and no chaos appears as clearance decreases. It is observed from the obtained power spectra that peak amplitude of vibration always appear in the spectrum only at the ball passage frequency (BPF). The contact force significantly fluctuates as the internal radial clearance changes from 6mm to 12 mm, the corresponding response changes as sub-harmonic to onset of chaos. For these responses, the hidden danger is periodicity.

Changqing and Qingyu (2006) have developed the dynamic model of ball bearings with internal clearance and waviness. Dynamic model is presented and dynamic properties of rotor system supported by ball bearings under the effects of both internal clearance and bearing running surface waviness. The ball bearing model includes the high-speed effects of ball centrifugal force and gyroscopic moment. The effects of clearance, waviness, preload and radial force on the nonlinear stability and vibration behaviour of a rotor bearing system at high speed was investigated. It is shown that the clearance, axial preload and radial force play a significant role in affecting the system stability. The effect of outer race waviness on cage speed variation is more considerable than that of inner race and ball waviness. The cage speed is determined by the orbital speed of balls. It was concluded that

1. When the axial preload is less than the critical value, the periodic solution loses the stability and the peak-to peak amplitudes of cage speed and axial and radial displacement have a dramatic increase.

2. The principal frequency of cage speed is a basic vibration frequencies component of system. It could be far less than the ball passage frequency as the system response is unstable or the radial load exists.

3. Effect of clearance on system stability is significant, as loses stability increases with an increase in clearance value. As the clearance increases, the radial peak-to-peak amplitude decreases while in axial peak-to-peak amplitude remains unchanged. Furthermore, the maximum cage speed decreases with an increase in axial preload and clearance.

4. The critical axial preload increases with radial load. Later on Changqing and Qingyu (2006) have also studied on dynamic Model of Ball Bearings with Internal Clearance and Waviness. In the paper investigation was done on dynamic stability and vibration characteristics of a rotor bearing system. The effects of both the clearance between the balls, races and the waviness on

bearing running surface are taken into account. Also, the model includes the high speed effects of the ball centrifugal force and gyroscopic moment. The cage speed is determined by the orbital speed of balls. They have shown that the proposed analysis is more reasonable than their numeric analysis, especially at high speed.

Mori et al. (2006) have investigated the prediction of spalling on a ball bearing by applying the discrete wavelet transform to vibration signals. The discrete wavelet transform (DWT) is applied to vibration signals to predict the occurrence of spalling in ball bearings. They concluded that impulsive responses appear in the vibration signal before spalling takes place, occurring when a ball rolls over the pre-spalling part of the raceway in the outer ring. The DWT of the vibration signals is a sensitive index of the impulsive responses. So as the impulsive responses increase as the occurrence of spalling comes near. The methodology presented in this paper can be easily applied to in-process monitoring system.

Gallina et al. (2006) have presented on application of coupling between Response Surface Methodology (RSM) and Monte Carlo Simulation in the field of dynamic analysis of mechanical structures. The error introduced by using an approximated meta model instead of the real model for the Monte Carlo Simulation has been analyzed and a solution has been proposed to overcome the problem. Later on Kankar et al. (2009) have reported the fault diagnosis of a rotor bearing system using response surface method. In this paper response surface method (RSM) is utilized to analyze the effects of design and operating parameters on the vibration signature of a rotor-bearing system. Distributed defects are considered such as internal radial clearance and surface waviness of the bearing components. They concluded that:

1. Nonlinear dynamic responses are found to be associated with large internal radial clearance and distributed defects. It is shown that the system exhibit dynamic behaviors that are extremely sensitive to small variations of the system parameters, such as internal radial clearance and ball waviness. The system shows periodic nature, when ball waviness is at its maximum level.

2. When the ball waviness is at its minimum level, the peak amplitude of vertical displacement response appears at ball passage frequency (ω_{bp}), while for horizontal displacement response peak amplitude of vibration appears at wave passage frequency (ω_{wp}) except when inner race waviness is at minimum level. When the ball waviness is at its maximum level then the peak amplitude of vibration appears at $i\omega_{wp} \pm j\omega_{ball}$ for both horizontal and vertical displacement

response, where *i, j* are integers

Abbasion et al. (2007) have reported the rolling element bearings multi-fault classification based on the wavelet denoising and support vector machine. For rolling bearing fault detection, it is expected that a desired time–frequency analysis method has good computational efficiency and has good resolution in both time and frequency domains. The point of interest of this investigation is the presence of an effective method for multi-fault diagnosis in such systems with optimizing signal decomposition levels by using wavelet analysis and support vector machine (SVM). They concluded that by using SVM classifier, Vibration data from bearings were denoised using discrete Meyer wavelet. Using the data from this procedure required parameters for classification of rolling bearing faults were found. The data were trained using SVM network. Some of the test data were examined to check correctness and accuracy of the algorithm and results showed 100% accuracy in fault detection.

Arslan and Aktürk (2008) have investigated the Rolling element vibrations caused by local defects. The investigation of the rolling element vibrations for an angular contact ball bearing with and without defects is done. They did their experimentation with a computer simulation program. Additionally, the effect of localized defects on running surfaces (i.e., inner ring, outer ring, and ball) on the vibration of the balls is investigated. Results are presented in time and frequency domains. Characteristic defect frequencies and their components can be seen in the frequency spectra of rolling element vibrations. Investigation of frequency spectrum for the outer race and inner race surfaces with defect showed that the dominant frequency peaks can be seen on first lower and upper sidebands of upper harmonics of the outer ring BPF, inner ring BPF. Resonance occurs in harmonics of the outer ring and inner ring BPFs and in some of the sidebands close to the shaft's natural frequency. It was concluded that by using the simulation model, defection of the defect in ball bearing elements can be identified.

Rafsanjani et al. (2009) have studied the nonlinear dynamic modeling of surface defects in rolling element bearing systems. Various surface defects due to local imperfections on raceways and rolling elements are introduced. The contact forces of each rolling elements has described according to non linear Hertzian contact deformation and effect of the internal radial clearance has taken into the account. The peak-to-peak frequency response of the system for each case is obtained and the basic routes to periodic, quasi-periodic and chaotic motions for different internal radial clearances are determined. It was investigated that location of defect at

small clearance affects the frequency at which the jump occurs. For outer race defect the peaks occurs at low shaft speeds while in the case of inner race and rolling element defect of the response peaks occurs then speed increases. The peak frequencies are different in each case.

Karacay and Akturk (2009) have presented the experimental diagnostics of ball bearings using statistical and spectral methods. Time domain analysis of vibration signature such as peak-to-peak amplitude, root mean square, Crest factor and kurtosis indicates defects in ball bearings. However, these measures do not specify the position and nature of the defects. Vibration signatures produced are recorded and statistical measures are calculated during the test. When anomalies are detected in the statistical measures, vibration spectra are obtained and examined to determine where the defect is on the running surfaces. Spectrum analyses are conducted at specified test durations in order to predict defect locations. In this study, they have also observed that when the defect size increases, the vibration magnitude and the severity also increase. However, it is not possible to find a general correlation between the defect size and the amplitude of the vibration. This is partially because the characteristic of the vibrations varies from system to system.

Su et al. (2010) have studied the rolling element bearing faults diagnosis based on optimal Morlet wavelet filter and autocorrelation enhancement. When localized fault occurs in a bearing, the periodic impulsive feature of the vibration signal appears in time domain and the corresponding bearing characteristic frequencies (BCFs) emerge in frequency domain. They investigated that new hybrid method based on optimal Morlet wavelet filter and autocorrelation enhancement algorithm for bearing fault diagnosis. The optimal Morlet wavelet filter can be used to eliminate the interfering vibration signal resulting from other sources and extract adequately the impulsive feature of a defective bearing. The SNR of the filtered signal obtained by using the optimal wavelet filter is increased significantly. In order to further reduce the in-band residual noise, autocorrelation enhancement algorithm is adopted. The proposed method is employed to the simulated signal and the real bearing vibration signals under different conditions, such as normal, inner-race fault and outer-race fault. There are only several single spectrum lines left in the enhanced autocorrelation envelope power spectrum. The proposed method can be conducted in an almost automatic way, with the minimal possible degree of user intervention.

Trendafilova (2010) has presented the automated procedure for fault detection and identification of ball bearing damage using multivariate statistics and pattern recognition. This study is based on pattern recognition and principal components analysis of the measured vibration signals. The signals recorded in the form of applying a wavelet transform in order to extract the appropriate high frequency (detailed) area needed for ball bearing fault detection. Pattern recognition (PR) procedure is used to recognise between signals coming from healthy bearings and those generated from different bearing faults. Four different categories of signals are considered, no fault signals (from a healthy bearing), inner race fault, outer race fault and rolling element fault signals. The PR procedure uses the first six principal components extracted from the signals after a proper principal component analysis (PCA). In this work a modified PCA is suggested, which is much more appropriate for categorical data. The combination of the modified PCA and the PR method ensures that the fault is automatically detected and classified to one of the considered fault categories. The method does not require the determination of the specific fault frequencies. Once the signal filtering is done and the PC's are found the PR method automatically gives the answer if there is a fault present.

Patil et al. (2010) have developed the theoretical model to predict the effect of localized defect on vibrations associated with ball bearing. The contacts between the ball and the races are considered as non-linear springs. The contact force is calculated using the Hertzian contact deformation theory. The results is presented in the form of time domain and frequency domain. Experimentation was worked on 6305 deep groove ball bearing. They concluded that amplitude level of vibrations in case of outer race defect is more than that for the inner race defect and the ball defect. It was also predicted from the model that the amplitude of vibration increases with the increase in the defect size and same is observed through experimentation.

Tomovic et al. (2010) have studied the vibration response of rigid rotor in unloaded rolling element bearing. By the application of the defined modal, the parametric analysis of the effect of internal radial clearance value and number of rolling elements influence on rigid rotor vibrations in unloaded rolling element bearing was performed. They concluded that the BPF linearly increases with the increase of number of rolling elements. This increase is more pronounced with the lower values of ratio between diameter of rolling elements and cage pitch diameter (d_b/d_c). With the increase of the internal radial clearance, the value of amplitude

increases linearly. The increase gets much bigger as the total number of rolling elements decreases.

Laniado-Jacome et al. (2010) have studied the sliding between rollers and races in a roller bearing with a numerical model for mechanical event simulations. For each roller, a rolling zone can be defined in which local sliding (computed between two consecutive time steps) is negligible. According to the simulations, they concluded that the rolling zone is practically the same for all the rollers in the same simulation. This rolling zone is smaller than the corresponding load zone. Rolling zones and load zones are angularly centered with respect to each other. Analytical model of Harris–Jones was implemented. They also investigated that the numerical model has revealed an absence of sliding within the load zone. The zone where the sliding factor has values near zero is called rolling zone. From the results of the simulations, they also investigated that by increasing the speed of rotation, the level of sliding decreases in average, but the rolling zone is more difficult to recognize.

Kankar et al. (2010) have investigated the fault diagnosis of ball bearings using machine learning methods. This study is focused on fault diagnosis of ball bearings using artificial neural network (ANN) and support vector machine (SVM). The specific defects are considered as crack in outer race, inner race with rough surface and corrosion pitting in balls. A comparative experimental study of the effectiveness of ANN and SVM is carried out. The results show that the machine learning algorithms mentioned above can be used for automated diagnosis of bearing faults. It was concluded that the accuracy of SVM is better than of ANN. Both the machine learning methods give less accuracy to correctly predict the bearing condition with combined bearing component fault but though results obtained from SVM are slightly better than ANN. Diagnosis of defect for applying condition based maintenance to prevent catastrophic failure and reduce operating cost.

Sawalhi and Randall (2011) have discussed the Vibration response of spalled rolling element bearings: Observations, simulations and signal processing techniques to track the spall size. This was investigated in this paper using vibration signatures of seeded faults at different speeds. The acceleration signals resulting from the entry of the rolling element into the spall and exit from it were found to be of different natures. The entry into the fault can be described as a step response, with mainly low frequency content, while the impact excites a much broader frequency that is impulse response. Two approaches were used to estimate the size of the fault.

1. The first approach utilizes octave band wavelet analysis to allow selection of the best band (or scale) to balance the two pulses with similar frequency content (joint treatment). Finally, the real cepstrum was used to find the average separation of the two pulses over a number of realizations.
2. In the second approach, a separate treatment of the step and impulse responses was performed so that they are equally represented in the composite signal. In this treatment, the pre-whitened signal is separated into two parts (step response and impulse response), which are processed separately.

While both methods gave a reasonable approximation of the size of the faults at different speeds, the second based on separate treatment is more accurate and less confusing, when presented in terms of mean and standard deviation.

Kankar et al. (2011) have investigated the rolling element bearing fault diagnosis using wavelet transform. In this is paper different approaches are applied for fault diagnosis of ball bearings having localized defects (spalls) on the various bearing components using wavelet-based feature extraction. Three artificial intelligence techniques are used for faults classifications, out of which these two are supervised machine learning (SML) techniques i.e. support vector machine (SVM), learning vector quantization (LVQ) and other one is an self-organizing maps (SOM). They concluded that the fault classification results show that the support vector machine identified the fault categories of rolling element bearing more accurately and has a better diagnosis performance as compared to the learning vector quantization and self-organizing maps. The responses observed for different fault condition of bearing shows that minimum Shannon Entropy is obtained for bearings with inner race fault. The results of faults classification with SVM (100%) are superior to LVQ and SOM. LVQ being the supervised version of SOM the classification accuracy obtained 89.3333%, which is better than SOM (74.6667%). The results show the potential application of these artificial intelligence techniques for developing effective maintenance strategies to prevent catastrophic failure.

Previous research articles have highlighted the advantages different technique used for detection of fault diagnosis. The key challenge to fault diagnosis is the improvement of diagnostics accuracy based on a given amount of information. Previous research articles, lot of work has been done on ball bearings and to identify the combination of defects in rolling

bearing elements is limited. Kankar et al. (2009) have investigated the combination effect of defects on ball bearing elements. A Little work has been reported on taper roller bearings. In the present investigation, a fault identification method based Fast Fourier Transformation (FFT) and Surface Response Method has been proposed on Taper Roller Bearing.

CHAPTER 3
PROBLEM FORMULATION

A lot of research is being directed towards rolling element bearings due to high speed and noise-sensitive applications like household appliance and automotive industry. These bearings act not only as structural elements but also as source of vibrations in rotor bearing systems. Research articles discussed in previous chapter have highlighted the advantages of different techniques used for detection of faults in bearings. The key challenge to fault diagnosis is the improvement of diagnostics accuracy based on a given amount of information. It is observed that lot of work has been done on ball bearings. A little work is reported on fault diagnosis in the taper roller bearings.

Recently, it is seen that the response surface method (RSM) is a new methodology for detecting the effects of defects on vibration response of rolling element bearings. Kankar et al. (2009) have investigated the effects of distributed defects on the ball bearing elements using RSM. The present study aims to identify the effects of localized defect like spall on amplitude of vibration using RSM. The combination effects of these defects on the taper roller bearings are also focused which is not done in most of the studies. This work attempts to analyze vibration responses of a horizontal rotor supported on taper roller bearings and also develop a fault identification system for rotor bearing system. The effects of severity of localized defects on the vibration response of bearings also need to be investigated. Experiments need to be conducted for obtaining vibration response of taper roller bearings with different fault conditions. Further, the present research work focus to enhance machinery reliability, availability, safety, and reduce maintenance costs.

CHAPTER 4

EXPERIMENTATION

Rolling element bearings are used in a wide variety of rotating machines from small hand-held devices to heavy duty industrial systems and are primary cause of breakdowns in these machines. In the rotating machines, one of the major concerns is fatigue failure in rolling element bearing components. When the repeatedly cycled stress on a surface in rolling contact it exceeds the endurance strength of the material, fatigue cracking of the surface occurs. This defect propagates and results in a large pit or spall on the surface of bearing components. A small fault in the bearing systems can quickly develop into a dangerous failure mode without any notable signs. Therefore, accurate machinery fault diagnosis is becoming of paramount importance to avoid catastrophic failure and human casualties.

The several vibration and acoustic measurement methods have been used for the detection of defects in rolling element bearings (Tandon and Choudhury, 1999). The vibration signals contain information of defective parts and a variety of vibration based techniques have been developed to monitor the condition of bearing. Vibration signals are analyzed using frequency domain analysis. Vibration signal is measured from the FFT signal processing techniques, are employed to extract the fault sensitive features to serve as the monitoring indices.

4.1 EXPERIMENTAL SETUP

It is necessary to predict the degradation of working conditions of bearings and trending of fault propagation to fully utilize the machine production capacity and to reduce the plant downtime. In the present study, experimentation is carried out on a rotor test rig as shown in Figure 4.1. Rotor test rig is constructed to study the dynamic behaviour of rotor supported on healthy and faulty bearings. The Taper Roller Bearing, 30304 A, has been used for present study. The rig is connected to a data acquisition system through proper instrumentation. One piezoelectric accelerometer has been used for picking up the vibration signals. Vibration responses for healthy bearings and bearings with faults are obtained for various speeds.

4.1.1 Test Rig

The test rig is a desktop rotor model, which consists of a rotor supported on taper roller bearings and driven by a DC motor. Firstly, the horizontal rotor is designed and manufactured having length of 760 mm and weight of 2.5 kg. The horizontal rotor is made of mild steel, grade of EN8. The rotor is driven by DC motor whose operating speed can be controlled. Two bearing brackets are used to hold and align the taper roller bearings inside the brackets. A flexible coupling (bellow type) has been used to connect rotor and motor. Four rubber shoes are fitted under the test rig model. Rubber shoes are used to absorb the vibration coming from the test rig. Test rig facilitates easy removal and replacement of the parts as shown in Figure 4.1.

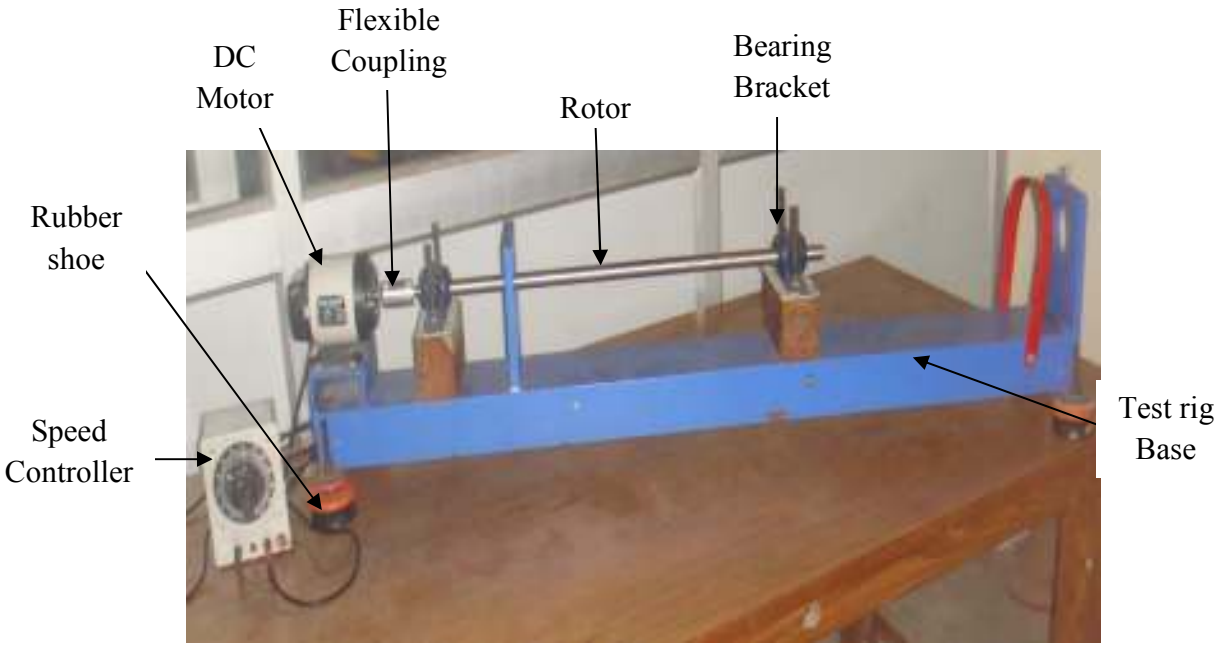

Figure 4.1 Experimental setup

4.1.2 Data Acquisition System

Data acquisition and analysis system consists of NV Gate software, which is designed in OR36 for quick data acquisition, review and storage. Data acquisition hardware consists of 16 analog input channels for simultaneous sampling. PCI bus provided high-speed data acquisition (52.4 k Samples/sec). Mechanical Tachometer is used to measure rotor speed. Piezoelectric accelerometers (353B34) having sensitively of .00101936 are used for picking up the vibration

signals. Measurement range of this accelerometer is 0.5-5000 Hz. In rotating machinery, the optimum signals are obtained from accelerometer located at the bearing housing. Therefore, accelerometer is fitted in vertical direction on the bearing housing. The diagram is shown in Figure 4.2.

Figure 4.2 Data acquisition system (OR36)

4.2 CHARACTERISTIC DEFECT FREQUENCIES OF ROLLING ELEMENT BEARINGS

When the rolling element set and the cage rotates with a constant rotational frequency of cage (ω_c), a parametrically excited vibration is generated and transmitted through the outer race. The characteristic frequency of this vibration is called the varying compliance frequency (*VC*). This is the frequency at which the rolling elements pass an observation point fixed on the outer race. In case of rotation, peak amplitude of vibration is generated at the varying compliance frequency and its harmonics (Kankar, 2011).

$$VC = N_r \text{ x } \omega_c \tag{4.1}$$

Defect in the outer race, inner race and rolling element generate vibrations at distinct frequencies. Assuming no slip and considering outer race to be stationary, the general form of the bearing defect frequency equations (Brändlein et al.,1999) are given below:

Cage rotational frequency

$$\omega_c = \frac{\omega_i\left(1-\frac{d}{D}\cos(\alpha)\right)}{2} \tag{4.2}$$

Rolling element passage frequency of Outer Race $$\omega_{ep} = \frac{N_r \omega_i \left(1 - \frac{d}{D}\cos(\alpha)\right)}{2} \quad (4.3)$$

(Defect frequency of outer race)

Rolling element passage frequency of Inner Race $$\omega_{ip} = \frac{N_r \omega_i \left(1 + \frac{d}{D}\cos(\alpha)\right)}{2} \quad (4.4)$$

(Defect frequency of inner race)

Rolling element passage frequency of Roller $$\omega_{rp} = \frac{\omega_i}{2}\frac{D}{d}\left(1 - \left(\frac{d}{D}\cos(\alpha)\right)^2\right) \quad (4.5)$$

(Roller spin frequency)

where ω_i is rotational frequency of inner race, d is the roller diameter, D is the pitch diameter, N_r is the number of rolling elements and α is the contact angle.

Theoretical Calculations of the above listed Frequencies at different speed (rpm) are given in Table 4.1

4.3 DYNAMICS RESPONSE OF TAPER ROLLER BEARING

In present work, the dynamic response of horizontal rotor supported by taper roller bearings (30304 A) has been studied. The excitation is due to varying compliance in case of healthy bearing and also due to localized defects on outer race, inner race and roller. The vibration responses due to horizontal rotor supported on healthy/faulty bearings are investigated. The effect of localized defect i.e spall in rolling element bearings have been considered and analyzed in detail for rotor bearing system. The present study characterizes the vibration frequencies resulting from taper roller bearing with localized defects existing in rolling elements, the harmonic frequencies resulting from the nonlinear load-deflection characteristics of the rolling element bearing and the sideband frequencies resulting from the defects interactions of the rolling element bearing.

Table 4.1 Theoretical Calculation of Frequencies at Different Speeds

Speed (rpm)	Rotational Frequency (Hz)				Varying compliance (Hz)	Defect Frequency (Hz)		
	ω_i	ω_e	ω_c	ω_r	VC	ω_{ip}	ω_{ep}	ω_{rp}
500	8.33	0	3.29	18.6	42.8	65.6	42.8	37.1
1000	16.7	0	6.58	37.1	85.5	131	85.5	74.3
1500	25	0	9.87	55.7	128.3	197	128	111
2000	33.3	0	13.2	74.3	171.6	262	171	149
2500	41.7	0	16.5	92.8	214.5	328	214	186
3000	50	0	19.7	111	256.1	393	257	223
3500	58.3	0	23	130	299	459	299	260
4000	66.7	0	26.3	149	341.9	524	342	297
4500	75	0	29.6	167	384.8	590	385	334
5000	83.3	0	32.9	186	427.7	656	428	371

4.3.1 Results and Discussion

The result obtained from Fast Fourier Transformation (FFT) for different defects are discussed below. In this experimentation, vibration responses are obtained from FFT, means response are in the form of Amplitude v/s Frequency.

1. Response of horizontal rotor supported on the healthy taper roller bearing

2. Response of horizontal rotor supported on the taper roller bearing with spall on outer race (spall size 1 mm).

3. Response of horizontal rotor supported on the taper roller bearing with spall on inner race (spall size 1 mm).

4. Response of horizontal rotor supported on the taper roller bearing with spall on roller (spall size 1 mm).

4.3.1.1 Response of horizontal rotor supported on the healthy taper roller bearing

When the rolling element set and the cage rotates with a constant rotational frequency of cage (ω_c), a parametrically excited vibration is generated and transmitted through the outer race. The characteristic frequency of this vibration equals (N_r x ω_c) and is called the varying compliance frequency (*VC*). This is the frequency at which the rolling elements pass an observation point fixed on the outer race. In case of rotation, peak amplitude of vibration is generated at the varying compliance frequency and its harmonics. The area where the rolling elements are still in contact with the races is generally referred as the loaded zone. A phenomenon closely related to parametric excitations is parametric resonance (Kankar, 2011). These excitations are unstable or large amplitude solutions that are not directly related to the natural frequencies of the system. Varying compliance frequency for the various speeds has been calculated in Table 4.1.

The vibration responses at the speed of 500 rpm and 1000 rpm are shown in Figures 4.3 and 4.4 respectively. For 500 rpm and 1000 rpm, it is clear that peak amplitude appears at twice of varying compliance frequency (2*VC*). Other peak appears at (13*VC*= 556.01 Hz) and (8*VC*= 684.32 Hz) for 500 and 1000 rpm respectively. The response at 1500 rpm is shown Figure 4.5. The peak amplitude appears at multiple of varying compliance frequency (2*VC*=256.62 Hz, 6*VC*=769.8 Hz). The frequency spectra at 2000 rpm is shown in Figure 4.6. The peak amplitude in vibration spectrum appears at multiple of varying compliance frequency (2*VC*=343.25 Hz, 5*VC*=858 Hz). Figure 4.7 shows that the peak response appears at multiple of varying compliance frequency (2.5*VC*=536.25 Hz, 3.5*VC*=750.75Hz) for 2500 rpm. The response at 3000 rpm is shown in Figure 4.8, the peak value appears at multiple of varying compliance frequency (2.5*VC*=640.25 Hz). The vibration response at the speed of 3500 rpm and 4000 rpm are shown in Figures 4.9 and 4.10. For 3500 rpm and 4000 rpm, it is clear that peak amplitude appears at multiple of varying compliance frequency (2.5 *VC*=747.5 Hz) and (2.5 *VC*=854.75 Hz) respectively. The response at 4500 rpm is shown Figure 4.11, the peak value appears at twice of varying compliance frequency (2*VC*=769.6 Hz). The speed at 5000 rpm is shown in Figure 4.12, the peak amplitude appears at varying compliance frequency (*VC*=427.7 Hz, 2*VC*=855.4 Hz). Peak amplitudes and their excitation frequency with respect to speeds is shown in Table 4.2.

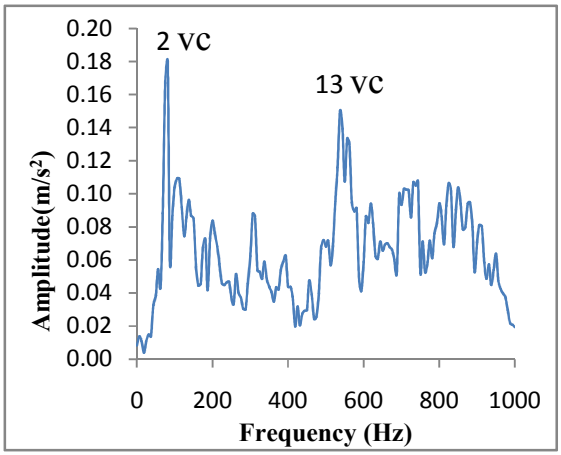

Figure 4.3 Response at 500 rpm (healthy bearing)

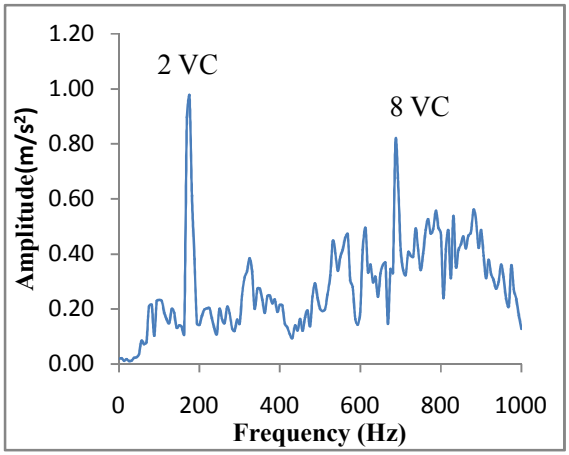

Figure 4.4 Response at 1000 rpm (healthy bearing)

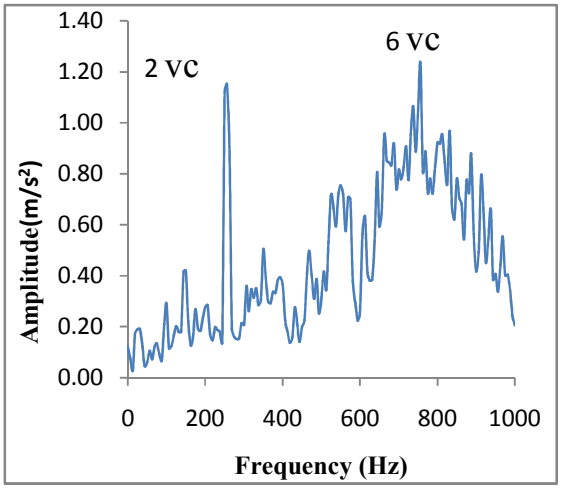

Figure 4.5 Response at 1500 rpm (healthy bearing)

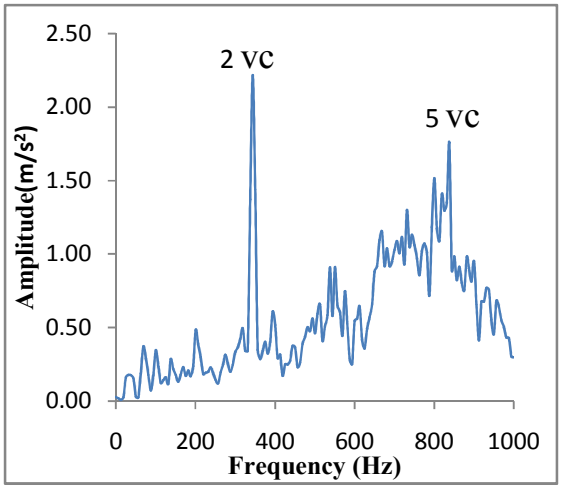

Figure 4.6 Response at 2000 rpm (healthy bearing)

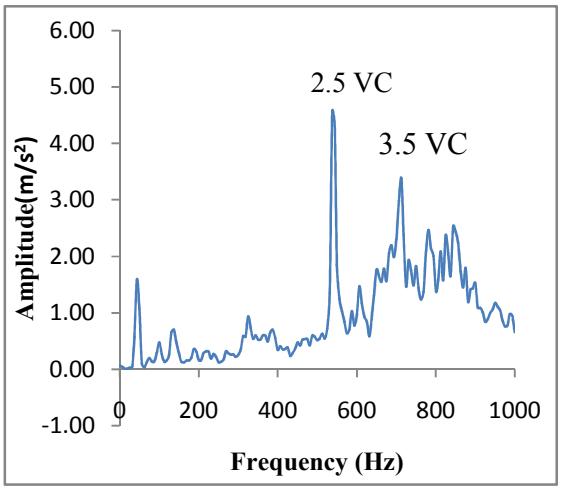

Figure 4.7 Response at 2500 rpm (healthy bearing)

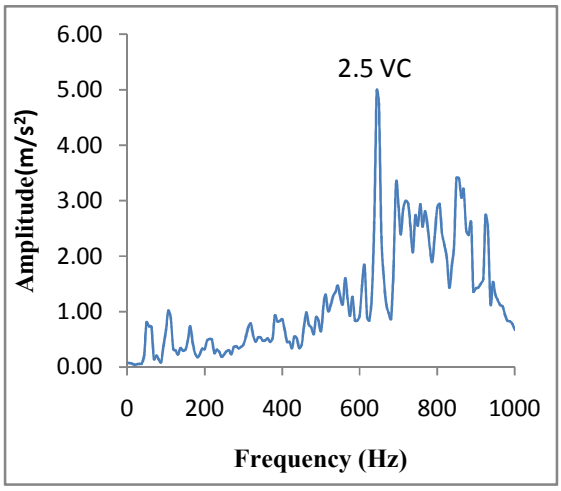

Figure 4.8 Response at 3000 rpm (healthy bearing)

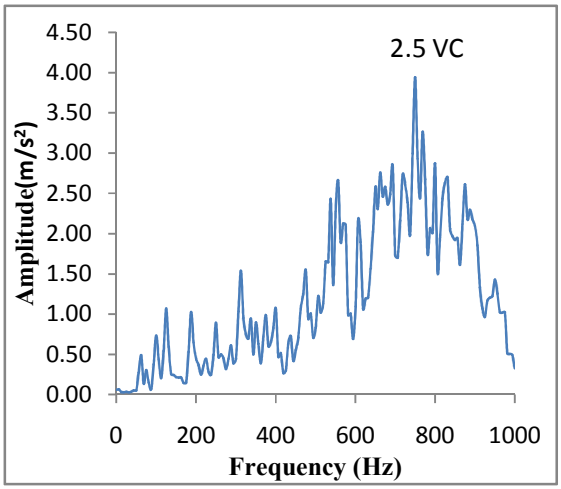

Figure 4.9 Response at 3500 rpm (healthy bearing)

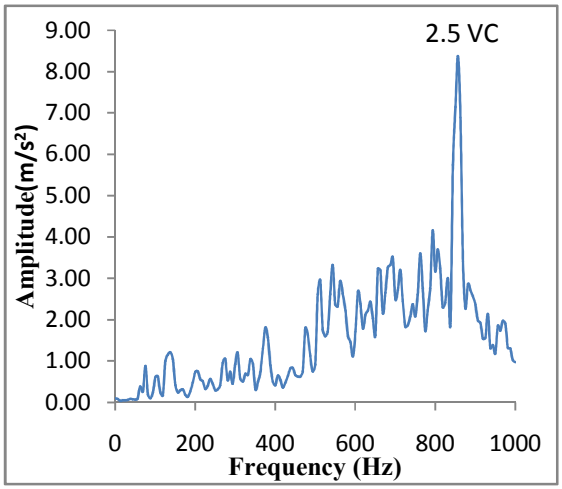

Figure 4.10 Response at 4000 rpm (healthy bearing)

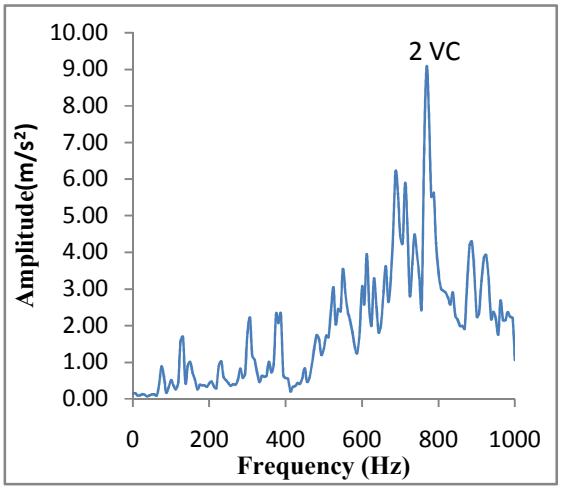

Figure 4.11 Response at 4500 rpm (healthy bearing)

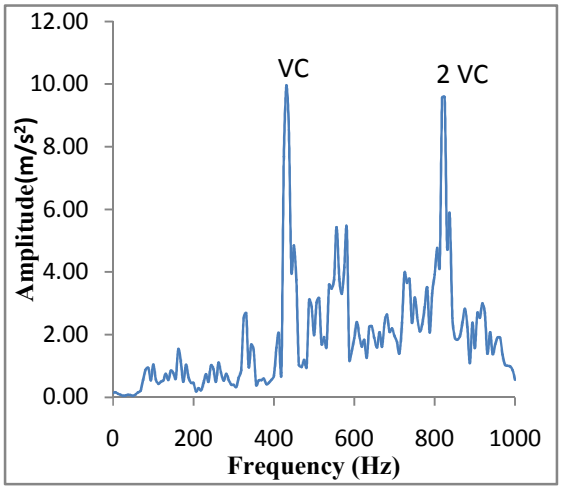

Figure 4.12 Response at 5000 rpm (healthy bearing)

Table 4.2 Summary of Healthy Bearing

Speed (rpm)	Peak Amplitude at	Harmonics of bearing spectrum at	Peak Amplitude (m/s^2)
500	$2VC$	$13VC$	0.179
1000	$2VC$	$8VC$	0.971
1500	$2VC$	$6VC$	1.533
2000	$2VC$	$5VC$	2.218
2500	$2.5VC$	$3.5VC$	4.556
3000	$2.5VC$	-	4.986
3500	$2.5VC$	-	3.847
4000	$2.5VC$	-	8.375
4500	$2VC$	-	9.064
5000	VC	$2VC$	9.952

4.3.1.2 Response of horizontal rotor supported on the taper roller bearing with spall on outer race (spall size 1 mm)

Spall is one of the most common localized defects present in the bearing. The vibrations response of outer race defect (spall) is excited, due to frequency when one point on outer raceway is damaged i.e ω_{ep} (rolling element passage frequency of outer race). Excitation in the outer race defect is due to rolling element passage frequency of outer race and sometimes excitation also interacting with cage frequency of the bearing (Kankar, 2011). In this study to observe the effect of spall on vibration responses, a set of results are obtained. The responses are obtained in frequency domain. FFT technique is used to understand the vibration response (amplitude v/s frequency). The amplitude of spall has been taken as 1mm, in this study.

Assuming no slip and considering outer race to be stationary, the general form of the Rolling element passage frequency of Outer Race is given in equation 4.6 (Brändlein et al., 1999). From this equation, rolling element passage frequency of outer race at various speeds has been calculated in Table 4.1.

Rolling element passage frequency of Outer Race $\omega_{ep} = \dfrac{N_r \omega_i \left(1 - \dfrac{d}{D}\cos(\alpha)\right)}{2}$ (4.6)

The vibration response of outer race defect (spall) is shown in Figure 4.13 at speed of 500 rpm, the peak amplitude appears at multiple of rolling element passage frequency of outer race ($2.5\omega_{ep}$=107 Hz, 17 ω_{ep}=727.6 Hz). The vibration responses at the speed of 1000 rpm, 1500 rpm and 2000 rpm are shown in Figures 4.14, 4.15 and 4.16. For 1000 rpm, 1500 rpm and 2000 rpm, it is clear that the peak amplitude appears at multiple of rolling element passage frequency of outer race ($2.5\omega_{ep}$). Other peaks appears at ($9\omega_{ep}$=769.5 Hz) and ($5\omega_{ep}$=855 Hz) for 1000 rpm and 2000 rpm respectively. The frequency spectra at 2500 rpm is shown in Figure 4.17, the peak amplitude appears as an interaction of rolling element passage frequency of outer race and cage frequency ($\omega_{ep} + 3\omega_c$=263.5 Hz, $2(\omega_{ep} + 3\omega_c)$ =527 Hz). The vibration responses at 3000 rpm and 3500 rpm are shown in Figures 4.18 and 4.19. The peak amplitude appears as an interaction of rolling element passage frequency of outer race and cage frequency ($\omega_{ep} + 3\omega_c$). Other peak appears at ($2(\omega_{ep} + 3\omega_c)$ =632.2 Hz) and ($1.5\ (\omega_{ep} + 3\omega_c)$ = 552 Hz) for 3000 rpm and 3500 rpm respectively. The frequency spectrum at 4000 rpm and 4500 rpm are shown in Figures 4.20 and 4.21 respectively. For 4000 rpm and 4500 rpm, it is clear that the peak amplitude appears at twice of rolling element passage frequency of outer race ($2\omega_{ep}$). The response at speed of 5000 rpm is shown in Figure 4.22, the peak amplitude appears at the rolling element passage frequency of outer race (ω_{ep}= 428 Hz, $2\omega_{ep}$=856 Hz). Peak amplitudes and their excitation frequency with respect to speeds is shown in Table 4.3.

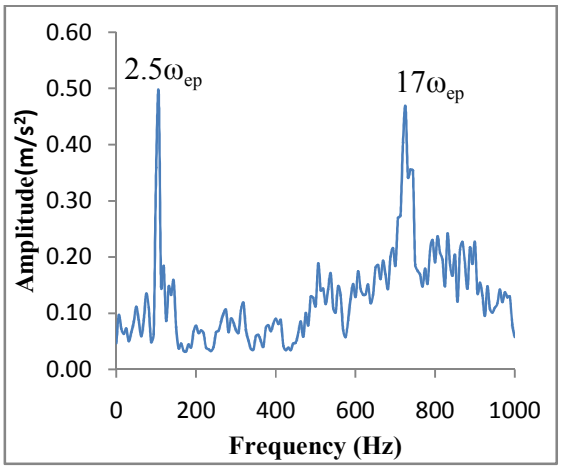

Figure 4.13 Response at 500 rpm(Spall on outer race)

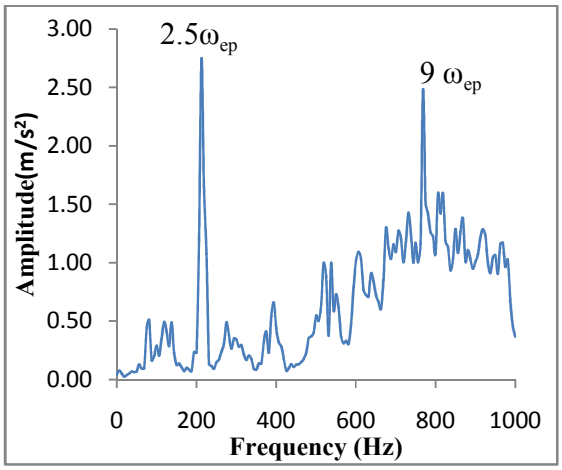

Figure 4.14 Response at 1000 rpm (Spall on outer race)

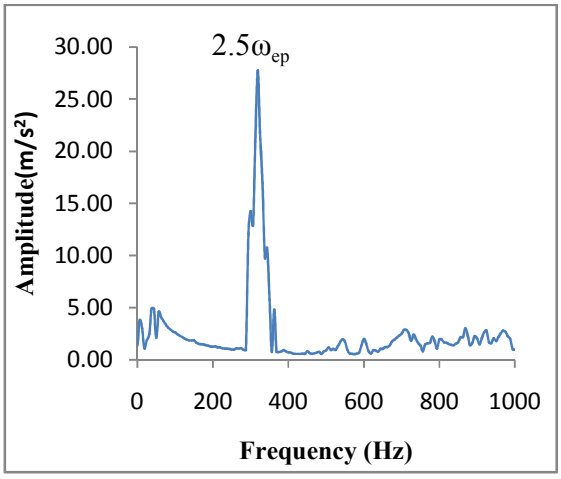

Figure 4.15 Response at 1500 rpm (Spall on outer race)

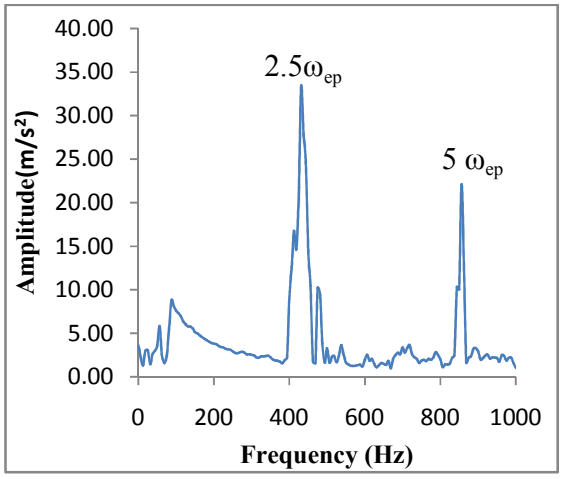

Figure 4.16 Response at 2000 rpm (Spall on outer race)

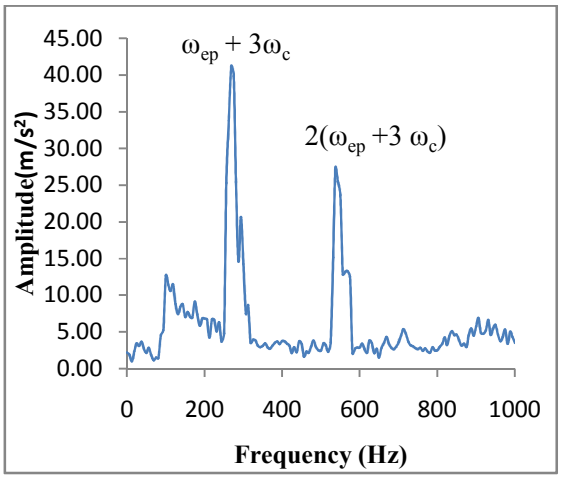

Figure 4.17 Response at 2500 rpm (Spall on outer race)

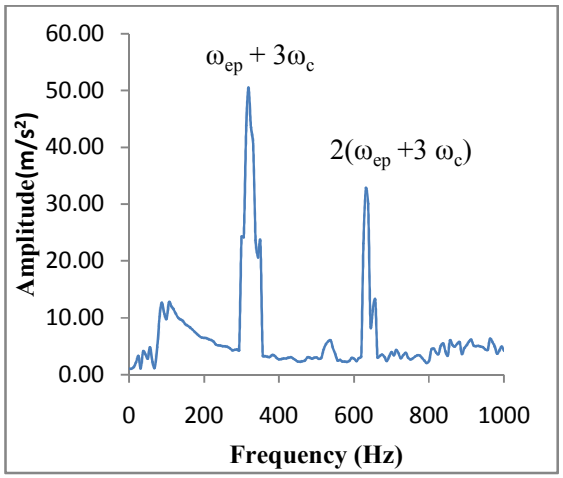

Figure 4.18 Response at 3000 rpm (Spall on outer race)

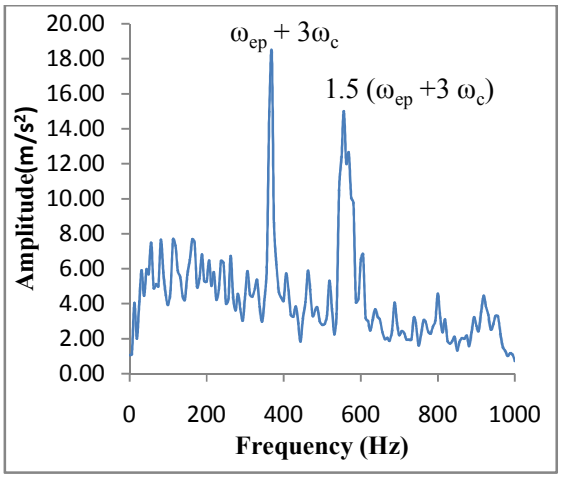

Figure 4.19 Response at 3500 rpm (Spall on outer race)

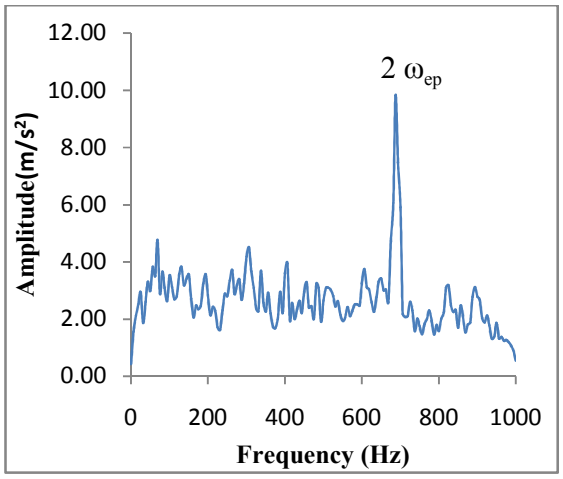

Figure 4.20 Response at 4000 rpm (Spall on outer race)

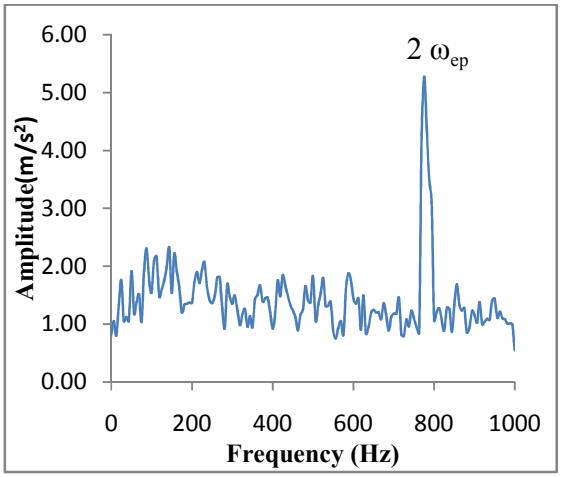

Figure 4.21 Response at 4500 rpm (Spall on outer race)

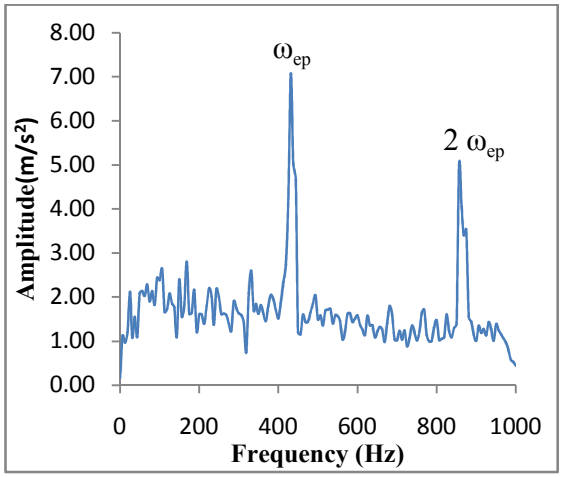

Figure 4.22 Response at 5000 rpm (Spall on outer race)

Table 4.3 Summary of Bearing with Spall on Outer Race

Speed (rpm)	Peak Amplitude at	Harmonics of Bearing Spectrum at	Peak Amplitude (m/s^2)
500	$2.5\omega_{ep}$	$17\omega_{ep}$	0.492
1000	$2.5\omega_{ep}$	$9\omega_{ep}$	2.748
1500	$2.5\omega_{ep}$	-	27.821
2000	$2.5\omega_{ep}$	$5\omega_{ep}$	33.473
2500	$\omega_{ep} + 3\omega_c$	$2(\omega_{ep} + 3\omega_c)$	41.229
3000	$\omega_{ep} + 3\omega_c$	$2(\omega_{ep} + 3\omega_c)$	50.514
3500	$\omega_{ep} + 3\omega_c$	$1.5(\omega_{ep} + 3\omega_c)$	18.332
4000	$2\omega_{ep}$	-	9.832
4500	$2\omega_{ep}$	-	5.273
5000	ω_{ep}	$2\omega_{ep}$	7.076

4.3.1.3 Response of horizontal rotor supported on the taper roller bearing with spall on inner race (spall size 1 mm)

The vibrations response of inner race defect (spall) is excited, due to frequency when one point on outer raceway is damaged i.e ω_{ip} (rolling element passage frequency of inner race).

Excitation in the inner race defect is due to rolling element passage frequency of inner race and sometimes excitation also interacting with cage frequency of the bearing (Kankar, 2011). Vibration response on the effect of spall having 1 mm on inner race is studied and set of results are obtained.

Assuming no slip and considering outer race to be stationary, the general form of the rolling element passage frequency of inner race equation is given in equation 4.7 (Brändlein et al., 1999). From this equation, rolling element passage frequency of inner race at various speeds has been calculated in Table 4.1.

Rolling element passage frequency of Inner Race $\omega_{ip} = \dfrac{N_r \omega_i \left(1 + \dfrac{d}{D}\cos(\alpha)\right)}{2}$ (4.7)

The vibration responses at speed of 500 rpm and 1000 rpm are shown in Figures 4.23 and 4.24 respectively. For 500 rpm and 1000 rpm, it is clear that the peak amplitude appears at twice of rolling element passage frequency of inner race ($2\omega_{ip}$). Other peak appears at ($11\omega_{ip}$= 721.6 Hz) and ($6\omega_{ip}$ =786 Hz) for 500 rpm and 1000 rpm respectively. The frequency spectra at 1500 rpm and 2000 rpm are shown in Figures 4.25 and 4.26, the peak value appears at twice of rolling element passage frequency of inner race ($2\omega_{ip}$). Other peak appears at ($5\omega_{ip}$ =985 Hz) and ($3\omega_{ip}$ =786 Hz) for 1500 rpm and 2000 rpm respectively. The response at speed 2500 rpm is shown in Figure 4.27. The peak amplitude appears at the multiple of rolling element passage frequency of inner race ($2\omega_{ip}$ =656 Hz). The vibration response at speed of 3000 rpm is shown in Figure 4.28, the peak amplitude appears as an interaction of rolling element passage frequency of inner race and cage frequency ($\omega_{ip} + 2\omega_c$ =432.4 Hz, $2(\omega_{ip} + 2\omega_c)$ =864.8 Hz). The frequency spectra at speed of 3500 rpm and 4000 rpm are shown in Figures 4.29 and 4.30 respectively. The peak amplitude appears as an interaction of rolling element passage frequency of inner race and cage frequency ($\omega_{ip} + 2\omega_c$). Other peak appears at ($1.5(\omega_{ip} + 2\omega_c)$ =757.5 Hz) and ($1.5(\omega_{ip} + 2\omega_c)$ =864.9 Hz) for 3500 rpm and 4000 rpm respectively. The vibration response at speed of 4500 rpm and 5000 rpm are shown in Figures 4.31 and 4.32 respectively. The peak amplitude appears as an interaction of rolling element passage frequency of inner race and cage frequency ($\omega_{ip} + 2\omega_c$ =649.2Hz) and ($\omega_{ip} + 2\omega_c$ =721.8Hz) for 4500 rpm and 5000 rpm respectively. Summary of excitation frequency and their peak amplitudes with respect to various speeds is shown in Table 4.4.

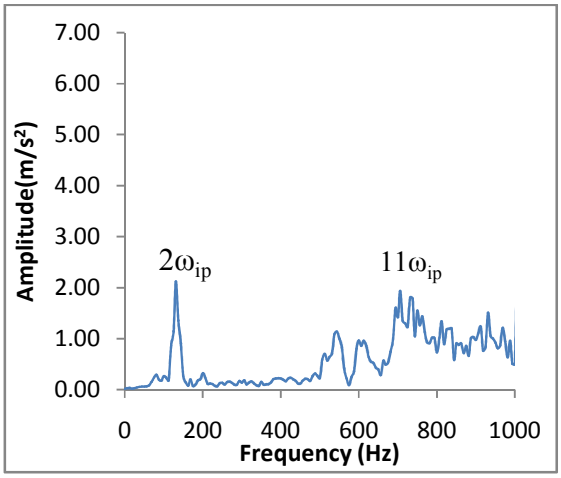

Figure 4.23 Response at 500 rpm (Spall on inner race)

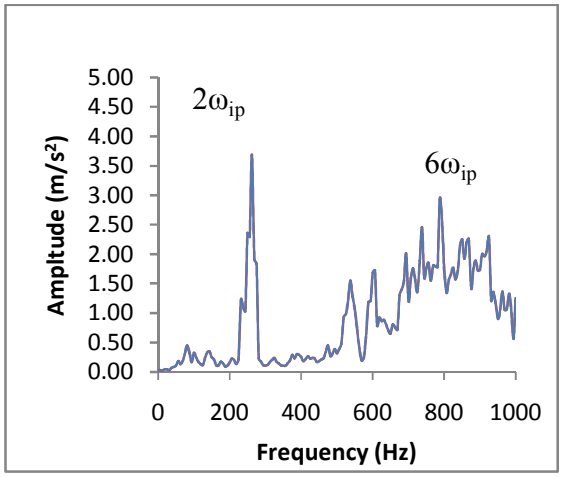

Figure 4.24 Response at 1000 rpm (Spall on inner race)

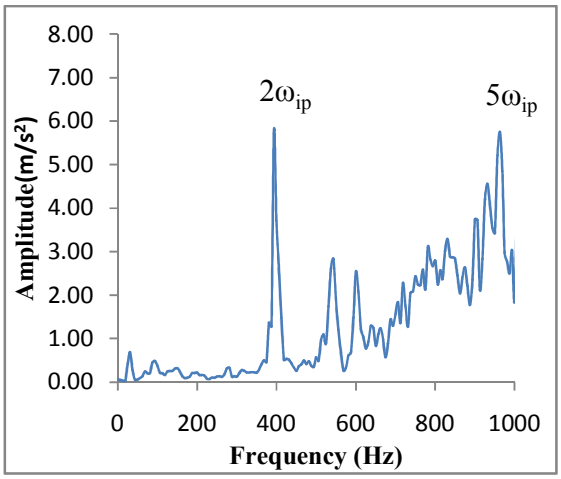

Figure 4.25 Response at 1500 rpm (Spall on inner race)

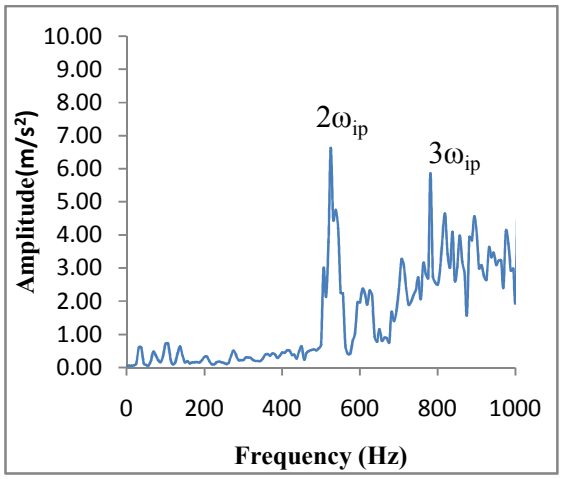

Figure 4.26 Response at 2000 rpm (Spall on inner race)

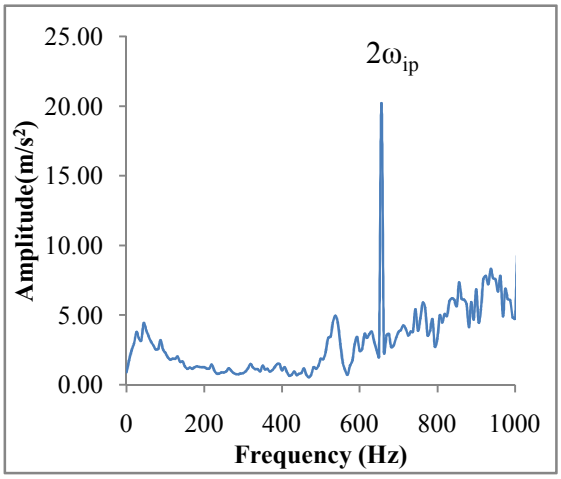

Figure 4.27 Response at 2500 rpm (Spall on inner race)

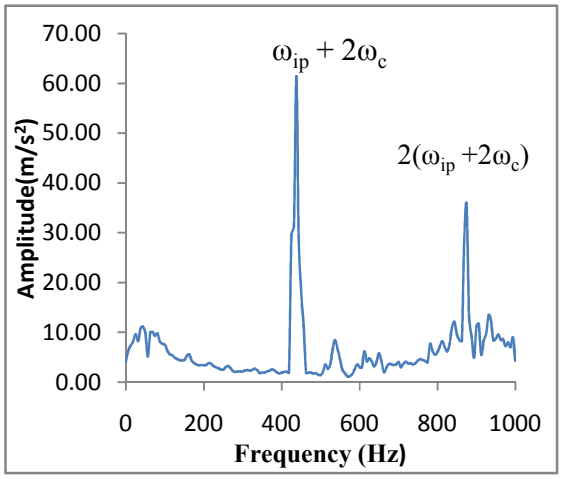

Figure 4.28 Response at 3000 rpm (Spall on inner race)

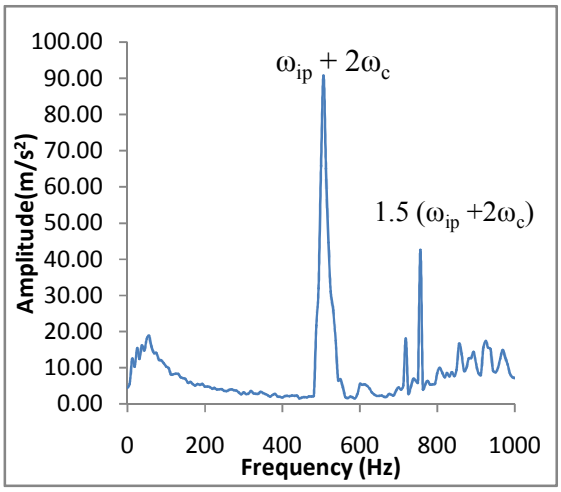

Figure 4.29 Response at 3500 rpm (Spall on inner race)

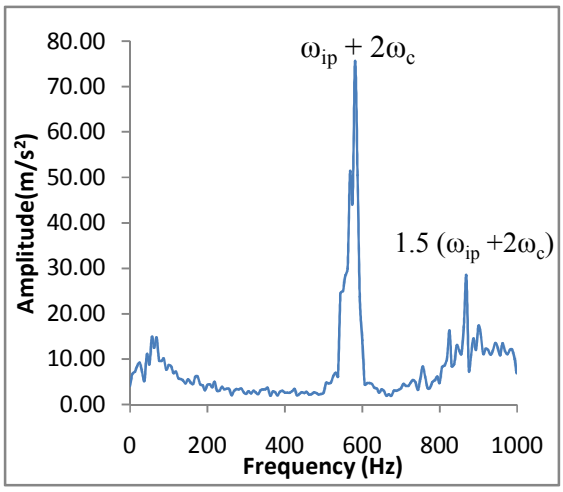

Figure 4.30 Response at 4000 rpm (Spall on inner race)

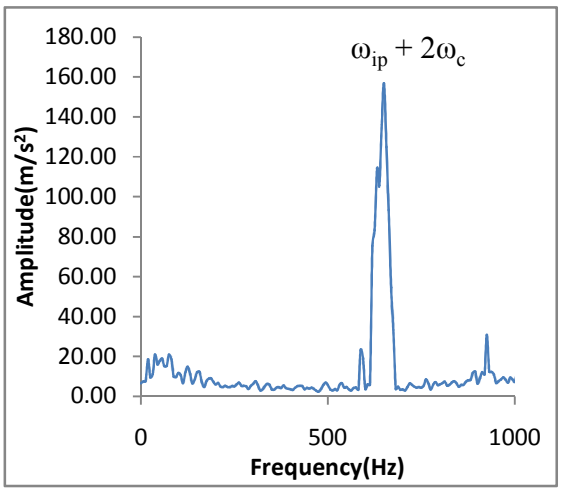

Figure 4.31 Response at 4500 rpm (Spall on inner race)

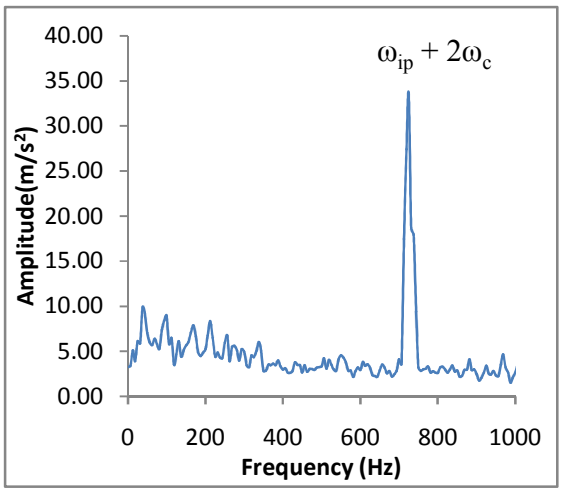

Figure 4.32 Response at 5000 rpm (Spall on inner race)

Table 4.4 Summary of Bearing with Spall on Inner Race

Speed (rpm)	Peak Amplitude at	Harmonics of Bearing Spectrum at	Peak Amplitude (m/s^2)
500	$2\omega_{ip}$	$11\omega_{ip}$	2.126
1000	$2\omega_{ip}$	$6\omega_{ip}$	3.651
1500	$2\omega_{ip}$	$5\omega_{ip}$	5.795
2000	$2\omega_{ip}$	$3\omega_{ip}$	6.622
2500	$2\omega_{ip}$	-	20.198
3000	$\omega_{ip}+ 2\omega_c$	$2(\omega_{ip}+ 2\omega_c)$	61.531
3500	$\omega_{ip}+ 2\omega_c$	$1.5(\omega_{ip}+ 2\omega_c)$	90.816
4000	$\omega_{ip}+ 2\omega_c$	$1.5(\omega_{ip}+ 2\omega_c)$	75.616
4500	$\omega_{ip}+ 2\omega_c$	-	157.018
5000	$\omega_{ip}+ 2\omega_c$	-	33.527

4.3.1.4 Response of horizontal rotor supported on the taper roller bearing with spall on roller (spall size 1 mm)

The vibrations response of roller defect (spall) is excited, due to frequency when one point on roller is damaged i.e. ω_{rp} (rolling element passage frequency of the roller). Excitation in the roller defect is due to rolling element passage frequency of the roller (Kankar, 2011). Vibration response on the effect of spall having 1 mm on roller is studied and set of results are obtained. Assuming no slip and considering outer race to be stationary, the general form of the Rolling element passage frequency of Roller is given in equation 4.8 (Brändlein et al., 1999). From this equation, rolling element passage frequency of roller at various speeds has been calculated in table 4.1.

Rolling element passage frequency of Roller $$\omega_{rp} = \frac{\omega_i}{2}\frac{D}{d}\left(1-\left(\frac{d}{D}\cos(\alpha)\right)^2\right) \quad (4.8)$$

The response of roller defect (spall) is shown in Figure 4.33, the peak amplitude appears at multiple of rolling element passage frequency of the roller ($2.5\omega_{rp}$ =92.75 Hz, $14\omega_{rp}$ =519.4 Hz). The frequency spectrum at speed 1000 rpm, 1500 rpm and 2000 rpm are shown in Figures 4.34, 4.35 and 4.36 respectively. For 1000 rpm, 1500 rpm and 2000 rpm, the peak amplitude

appears at multiple of rolling element passage frequency of the roller ($2.5\omega_{rp}$). Other peaks appears at ($10\omega_{rp}$ =743 Hz), ($7\omega_{rp}$ =777 Hz) and ($5\omega_{rp}$ =745 Hz) for 1000 rpm, 1500 rpm and 2000 rpm respectively. The vibration responses at speed 2500 rpm and 3000 rpm are shown in Figures 4.37 and 4.38 respectively. For 2500 rpm and 3000 rpm, it is clear that the peak amplitude appear at thrice of rolling element passage frequency of the roller ($3\omega_{rp}$). Other peaks appears at ($4\omega_{rp}$ =744 Hz) and ($4\omega_{rp}$ =892 Hz) for 2500 rpm and 3000 rpm respectively. The response at 3500 rpm is shown in Figure 4.39, the peak value appears at multiple of rolling element passage frequency of the roller ($2.5\omega_{rp}$ =650 Hz, $3\omega_{rp}$ =780 Hz). The vibration responses at speed of 4000 rpm and 4500 rpm are shown in Figures 4.40 and 4.41 respectively. For 4000 rpm and 4500 rpm, it is clear that the peak amplitude appears at twice of rolling element passage frequency of the roller ($2\omega_{rp}$). Other peak appears at ($2.5\omega_{rp}$ =835 Hz) for 4500 rpm. The response at 5000 rpm is shown in Figure 4.42, the peak amplitude appears at twice of rolling element passage frequency of the roller ($2\omega_{rp}$ =742 Hz). Summary of peak amplitudes and their excitation frequency with respect to various speeds is shown in Table 4.5.

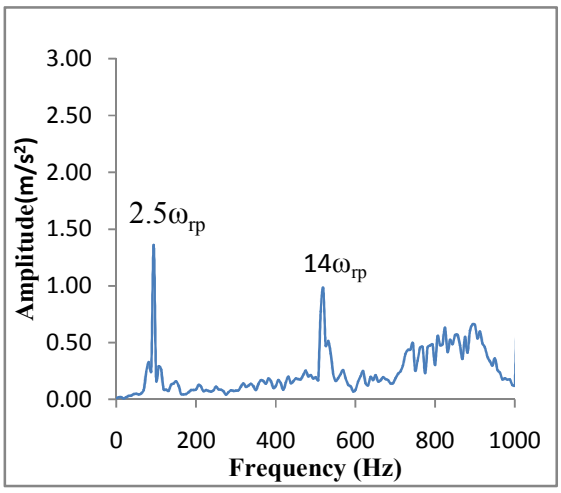

Figure 4.33 Response at 500 rpm (Spall on roller)

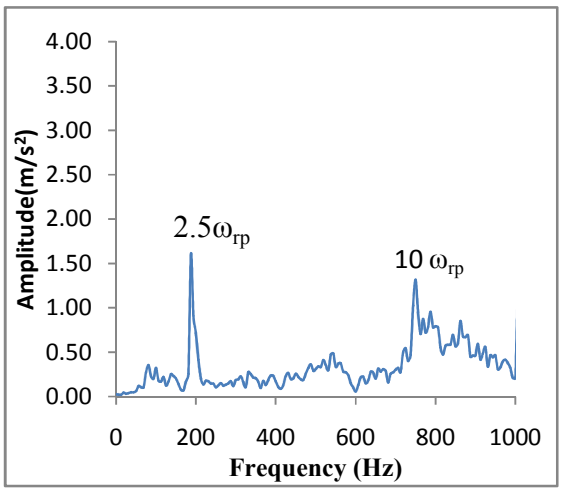

Figure 4.34 Response at 1000 rpm (Spall on roller)

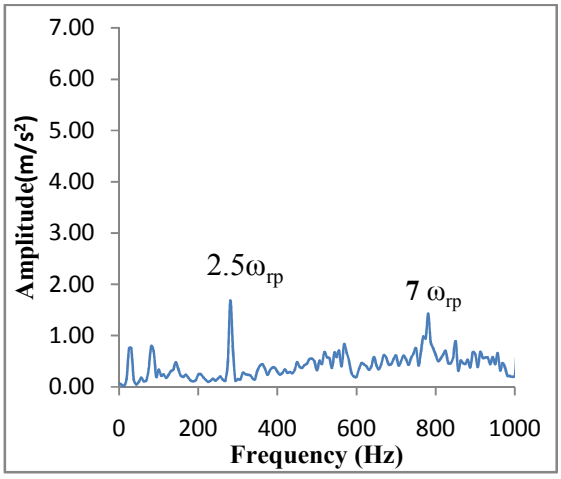

Figure 4.35 Response at 1500 rpm (Spall on roller)

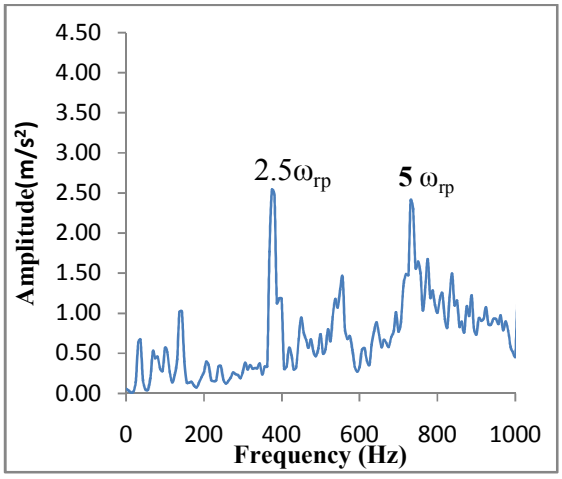

Figure 4.36 Response at 2000 rpm (Spall on roller)

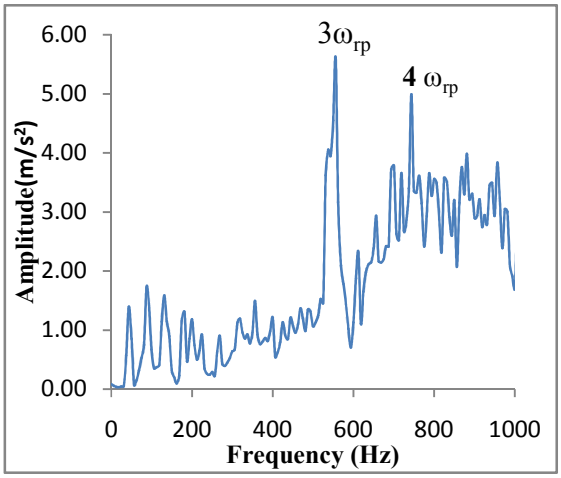

Figure 4.37 Response at 2500 rpm (Spall on roller)

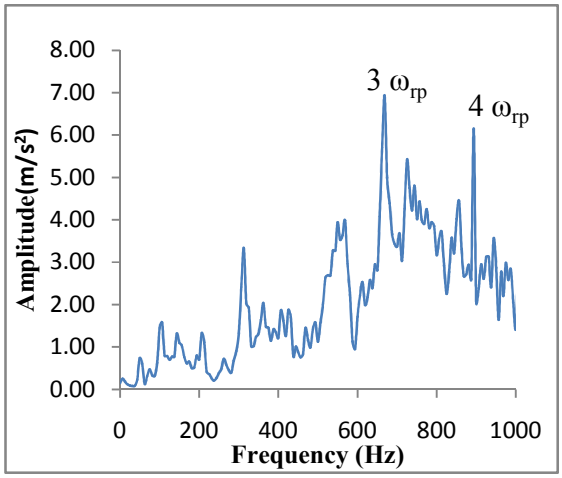

Figure 4.38 Response at 3000 rpm (Spall on roller)

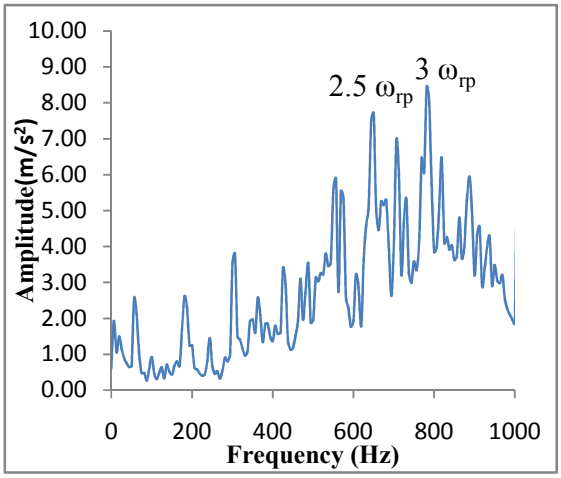

Figure 4.39 Response at 3500 rpm (Spall on roller)

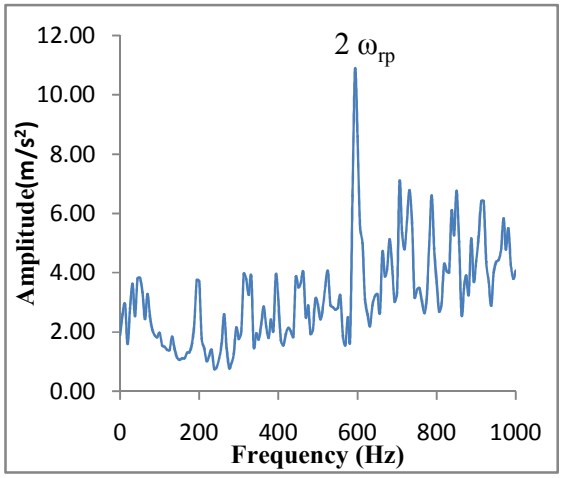

Figure 4.40 Response at 4000 rpm (Spall on roller)

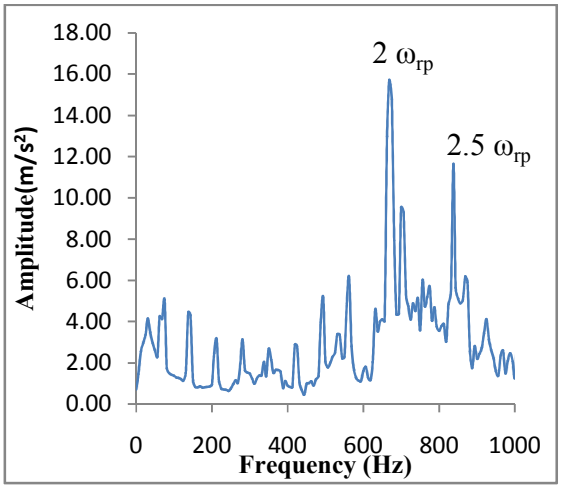

Figure 4.41 Response at 4500 rpm (Spall on roller)

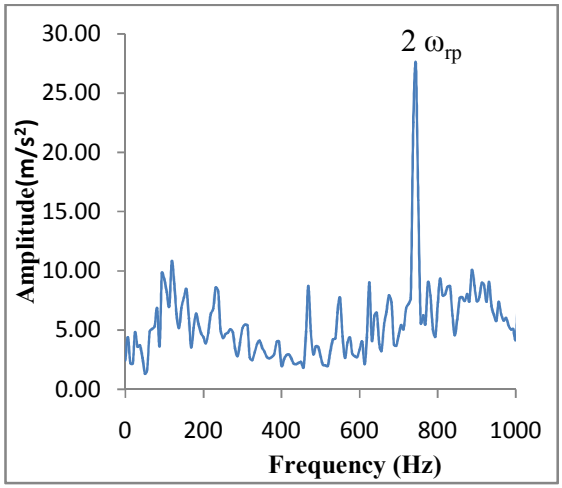

Figure 4.42 Response at 5000 rpm (Spall on roller)

Table 4.5 Summary of Bearing with Spall on Roller

Speed (rpm)	Peak Amplitude at	Harmonics of Bearing Spectrum at	Peak Amplitude (m/s^2)
500	$2.5\omega_{rp}$	$14\omega_{rp}$	1.361
1000	$2.5\omega_{rp}$	$10\omega_{rp}$	1.604
1500	$2.5\omega_{rp}$	$7\omega_{rp}$	1.692
2000	$2.5\omega_{rp}$	$5\omega_{rp}$	2.541
2500	$3\omega_{rp}$	$4\omega_{rp}$	5.598
3000	$3\omega_{rp}$	$4\omega_{rp}$	6.932
3500	$3\omega_{rp}$	$2.5\omega_{rp}$	8.447
4000	$2\omega_{rp}$	-	10.927
4500	$2\omega_{rp}$	$2\omega_{rp}$	15.729
5000	$2\omega_{rp}$	-	27.508

4.4 FAULT IDENTIFICATION OF TAPER ROLLER BEARING USING RESPONSE SURFACE METHODOLOGY (RSM)

The problem of predicting the degradation of working conditions of bearings and trending of fault propagation before they reach the alarm or failure threshold is extremely important in industries to fully utilize their machine production capacity and to reduce the plant downtime. Literature survey has revealed that most of the research on bearing faults has been carried out

considering single dimensional aspect (single factor affecting vibration response) of bearing faults such as fault in either of inner race, outer race or ball etc. Data generated using traditional method of research using single factor effect is valuable and detailed, but fails to indicate the effects of interactions between various test parameters (factors) on vibration response.

Therefore, for an efficient experimentation a systematic scientific approach is necessary to design and carry out the experimentation properly. A properly planned experimentation is of utmost importance for deriving clear and accurate conclusion/inferences from the experimental observations. Response Surface Methodology (RSM) is considered to be a very useful strategy for accomplishing these tasks. In general, RSM established the methods for drawing inferences from observations, when inferences are not exact but subject to variation.

The present study aims to identify effect of various faulty in Taper roller bearing components on the vibration response of a rotor bearing system. Faults on bearing components are considered as spall on outer race, inner race and roller. Experiments are carried out for healthy bearings and faulty bearings. Vibration responses for all cases are presented as FFT. RSM is used to find the effect of various localized bearing component faults on vibration responses and interactions between faults. Severe vibration conditions are determined by approximating amplitude of vibration using a series of polynomials using RSM.

4.4.1 Response Surface Methodology

The response surface methodology is a collection of mathematical and statistical techniques that are useful for modeling and analysis in applications, where a response interest is influenced by several variables and the objective is to optimize this response. RSM has been developed by Box and Wilson (1951) to explore the potential of statistical design in industrial experiments. The application of this methodology are used in a wide variety of industrial settings like chemical processes, semiconductor and electronics manufacturing, machining, metal cutting, and joining processes etc. RSM constructs polynomial approximations to build functional relationships between design variables and performances. The input variables are sometimes called independent variables or factors, and the performance measures or quality characteristics are called as responses. For the most response surface, the relationship between the response

variable of interest (y_0) and the factors ($x_1, x_2, \ldots, x_k$) may be described in the following second-order equation.

$$y_0 = f(x_0) = \beta_o + \sum_{i=1}^{n} \beta_i x_i + \sum_{i=1}^{n} \beta_{ii} x^2{}_i + \sum_{i=1, j>1}^{n} \beta_{ij} x_i x_j + \varepsilon \quad (4.9)$$

where ε represents the noise or error observed in the response y_0, β_0, β_i … are polynomial coefficients, and n is number of factors. Equation (4.9) can also be expressed in matrix form as :

$$Y_0 = X_0 B + \varepsilon \quad (4.10)$$

The method of least squares is used to estimate the polynomial coefficients in approximating polynomials such that minimize the sum of squares of the model errors. Then matrix B of polynomial coefficients can be obtained from the formula

$$B = \left(X_0{}^T X_0\right)^{-1} X_0{}^T Y_0 \quad (4.11)$$

The response surface analysis is done in terms of the fitted surface. Once a response surface model is obtained, statistical analysis technique such as analysis of variance (ANOVA) can be used to check the fitness of the model.

4.4.2 Experimentation

Rolling element bearings are of paramount importance to almost all forms of rotating machinery. Predicting the severe vibration conditions due to faults in bearings is extremely important in industries. In the present work, a test rig (experimental set up) as shown in Figure 4.1 is used with horizontal rotor supported on Taper Roller Bearings 30304 A. Various parameters of bearings used for the study are listed in Table 4.6.

In the present study, experiments are carried out to analyze effect of various bearing component defects on the vibration response of the rotor bearing system using response surface method. As a first step, the machine operated with healthy bearing to establish the base-line data. Then data are collected for different fault conditions. A variety of faults are simulated on the rig at 1000 rpm, 2500 rpm and 5000 rpm. RSM is used to find the effect of localized bearing component faults on vibration responses and interactions between faults. In order to perform response surface analysis to determine the combination of defects that gives the severe

vibration conditions, DOE is used with total 21 trial runs. Table 4.7 shows parameters used for DOE with their minimum and maximum level.

4.4.2.1 Surface defects

Spalls, pits and dents are the major forms of bearing damage. Fatigue cracking of the surface occurs, when the repeatedly cycled stress on a surface in rolling contact with another, exceeds the endurance strength of the material. This defect propagates and results in a large pit or spall on the surface of bearing components. Corrosion and oxidation pits, true/false brinnelling and hard particle contamination dents act as locations for incipient fatigue. This can cause bearing endurance to be shorter than that designed and may cause the rapid failure of the bearing. In this study, a defect (spall) has been considered on the outer race, inner race and rolling element as shown in Figure. 4.43.

(a) Inner Race with Spall **(b)** Outer Race with spall **(c)** Roller with spall

Figure 4.43 Faults considered in the bearing components

Table 4.6 Parameters of Bearing Used for Experiment

Parameter	**Value**
Taper Roller Bearing specification	30304 A
Outer race diameter	52 mm
Inner race diameter	20 mm
Mean Roller diameter	7.87 mm
Number of Rollers	13
Radial Load	25kN

Table 4.7 Parameters for DOE

Parameter Designation Symbols	Parameters	Minimum Level (0)	Maximum Level (2)
A	Inner Race with spall	0	2 mm
B	Outer Race with spall	0	2 mm
C	Roller with spall	0	2 mm
D	Speed of rotor	1000 rpm	5000 rpm

4.4.2.2 Response surface model establishment

This procedure begins with the identification of factors that affect the stability of the rotor bearing system. Each parameter affects the nature of the response in mutual interactions with other parameters as well as with separate factors.

Following bearing component faults are considered with rotor speed as factors that are influencing responses which are taken as peaks of vibration response in vertical direction.

A. Spall on inner race (Figure 4.43 (a))
B. Spall on outer race (Figure 4.43 (b))
C. Roller with spall (Figure 4.43 (c))
D. Speed of rotor

These four factors are selected with three levels. The upper and lower levels of each factor are defined in Table 4.7. In order to perform DOE to determine the condition that gives the severe vibration conditions, experiments are carried out in 21 trials with different set of bearings as listed in Table 4.9.

Table 4.8 Characteristic Frequencies

Characteristic Frequency	**Formula**		**Rotor Speed**	
		1000 RPM	**2500 RPM**	**5000 RPM**
Cage frequency (ω_c)	$\omega_c = \frac{\omega_i\left(1-\frac{d}{D}\cos(\alpha)\right)}{2}$	6.58 Hz	16.5 Hz	32.9 Hz
Varying compliance frequency (VC)	$VC = N_r \times \omega_c$	85.5 Hz	214.5 Hz	427.7 Hz
Rolling element passage frequency of inner race (ω_{ip})	$\omega_{ip} = \frac{N_r\omega_i\left(1+\frac{d}{D}\cos(\alpha)\right)}{2}$	131 Hz	328 Hz	656 Hz
Rolling element passage frequency of outer race (ω_{ep})	$\omega_{ep} = \frac{N_r\omega_i\left(1-\frac{d}{D}\cos(\alpha)\right)}{2}$	85.5 Hz	214 Hz	428 Hz
Roller spin frequency (ω_{rp})	$\omega_{rp} = \frac{\omega_i}{2}\frac{D}{d}\left(1-\left(\frac{d}{D}\cos(\alpha)\right)^2\right)$	74.3 Hz	186 Hz	371 Hz

Table 4.9 DOE Set and Results

Trial	Inner Race	Outer Race	Roller	Speed	Vibration Response
	A	**B**	**C**	**D**	**Peak Amplitude** (m/s^2)
1	0	0	0	1000	0.970
2	1	0	0	1000	3.651
3	2	0	0	1000	4.086
4	0	1	0	1000	2.748
5	0	2	0	1000	3.076
6	0	0	1	1000	1.604
7	0	0	2	1000	2.418
8	0	0	0	2500	4.566
9	1	0	0	2500	20.198
10	2	0	0	2500	29.094
11	0	1	0	2500	41.229
12	0	2	0	2500	27.871
13	0	0	1	2500	5.598
14	0	0	2	2500	6.417
15	0	0	0	5000	9.951
16	1	0	0	5000	33.526
17	2	0	0	5000	38.094
18	0	1	0	5000	7.071
19	0	2	0	5000	30.282
20	0	0	1	5000	27.508
21	0	0	2	5000	35.674

4.4.3 Results and Discussion

The vibration response for healthy and faulty bearings at speed 1000, 2500 and 5000 rpm have been shown in form of frequency spectra as shown in Figures 4.44, 4.45 and 4.46 respectively. Figure 4.44 shows the vibration response plots without and with localized defects on bearing components at rotor speed 1000 rpm. For healthy bearings, the peak amplitude of vibration

excitation appears at the multiple in frequency spectra as shown in Figure 4.44 (a). In presence of spall on inner race, the peak amplitude of vibration appears in the spectrum at super harmonic of rolling element passage frequency of inner race, ($2\omega_{ip}$) and ($3\omega_{ip}$) as shown in Figure 4.44 (b). Figure 44.4 (c) shows the response with spall on outer race. The peak amplitude of vibration appears at the multiple of rolling element passage frequency of outer race, ($2.5\omega_{ep}$) and ($3\omega_{ep}$) respectively. Next trial is considered with spall on roller. Exciting frequency appears at multiple rolling element passage frequency of roller and its harmonics in frequency spectra as shown in Figure 4.44 (d).

The vibration response plots shown (Figure 4.45) without and with localized defects on bearing components at rotor speed 2500 rpm. The vibration response for healthy bearings is shown Figure 4.45 (a), the peak amplitude of vibration excitation appears at multiple of varying compliance frequency (2.5 *VC*). In presence of spall on inner race, the peak amplitude of vibration appears in the spectrum at twice of rolling element passage frequency of inner race at ($2\omega_{ip}$) as shown in Figure 4.45 (b). Figure 44.5 (c) shows the response with spall on outer race. The peak amplitude of vibration appears in the response as an interaction of rolling element passage frequency of outer race and cage frequency at (ω_{ep}+ $3\omega_{c}$) with spall size 1mm. For spall size 2 mm, peak in vibration spectra appears at multiples of rolling element passage frequency of outer race at ($4\omega_{ep}$). Next trial is considered with spall on roller. Exciting frequency appears at rolling element passage frequency of roller and its harmonics in frequency spectra as shown in Figure 4.45(d).

Vibration responses of a horizontal rotor supported on healthy and faulty bearings at 5000 rpm have been observed as shown in Figure 4.46. When healthy bearings without any defect have been taken, the peak excitation occurs at Varying Compliance frequency (*VC*) due to parametric excitation as shown in Figure 4.46 (a). While bearing with the inner race defect (spall), have shown the peak excitation in vibration spectra as the interaction of rolling element passage frequency of inner race and cage frequency as shown in Figure 4.46 (b). The other defect in bearing components as outer race and the peak amplitude appears at rolling element passage frequency of outer race (ω_{ep}) and its harmonics as shown in Figure 4.46 (c). Figure 4.46 (d), shows the frequency spectra of spall on roller, the peak amplitude appears at the twice of rolling element passage frequency of roller ($2\omega_{rp}$).

Table 4.9 shows for the trials 1 to 21 peak amplitude of vibration appears in the spectrum for acceleration response. Through the experiments, the polynomials *f(x)* is approximated by the design parameters (A, B, C and D). The final functions of response surface model is shown in Equation 4.9:

The approximated polynomial for acceleration response is;

$$(\text{AMPLITUDE})^{-0.04} = +1.07335 - 0.068242 \times \text{INNER RACE} - 0.099467 \times \text{OUTER RACE} - 0.044289 \times \text{ROLLER} - 8.17625E\text{-}005 \times \text{SPEED} + 5.28226E\text{-}006 \times \text{OUTER RACE} \times \text{SPEED} + 3.12646E\text{-}005 \times \text{ROLLER} \times \text{SPEED} + 0.020353 \times \text{INNER RACE}^2 + 0.049517 \times \text{OUTER RACE}^2 + 1.00389E\text{-}008 \times \text{SPEED}^2 - 1.40081E\text{-}005 \times \text{OUTER RACE}^2 \times \text{SPEED} + 3.78509E\text{-}009 \times \text{OUTER RACE} \times \text{SPEED}^2 - 5.57867E\text{-}009 \times \text{ROLLER} \times \text{SPEED}^2 \quad (4.9)$$

The performance prediction of vibration amplitude response has been shown in Figure 4.47. The actual and predicted values of response are very close and verify fitness of polynomial for response.

In order to verify whether the obtained polynomials are valuable or not, the variance analysis and F-ratio test on them have been performed. Analysis of variance for acceleration response is shown in Table 4.10. The model F-value of 19.74 shows, the model is significant. Values of "Prob>F" less than 0.0500 indicate model terms are significant. In this case A, B, A^2, D^2, B^2D, CD^2 are significant model terms. After testing the polynomials using ANOVA, these are used to analyze the relation between factors and their corresponding responses. Response surfaces for acceleration responses are developed as shown in Figure 4.48 to 4.53.

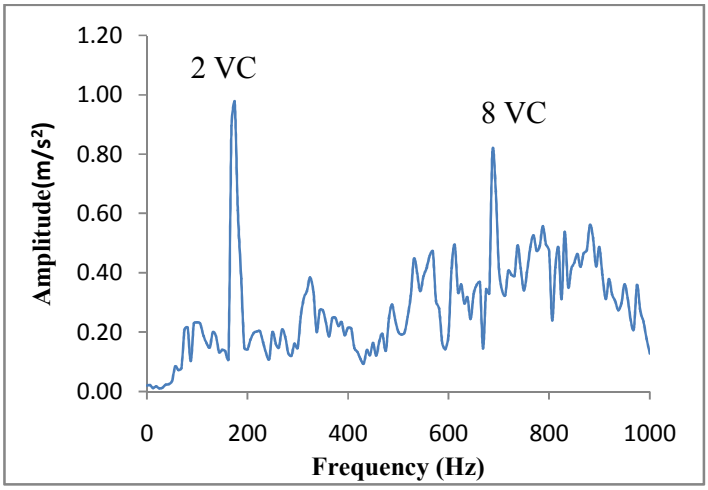

(a) Healthy Bearing

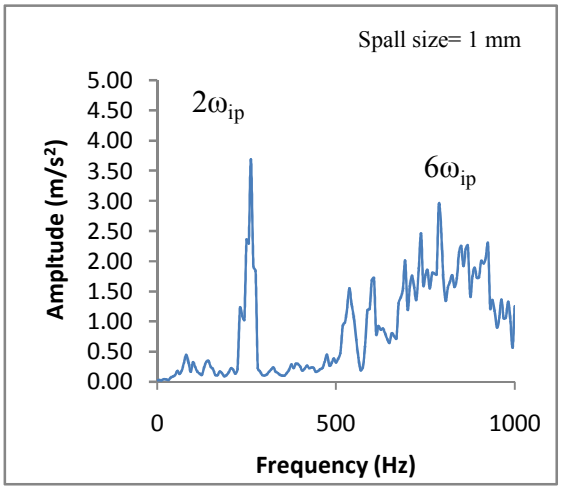

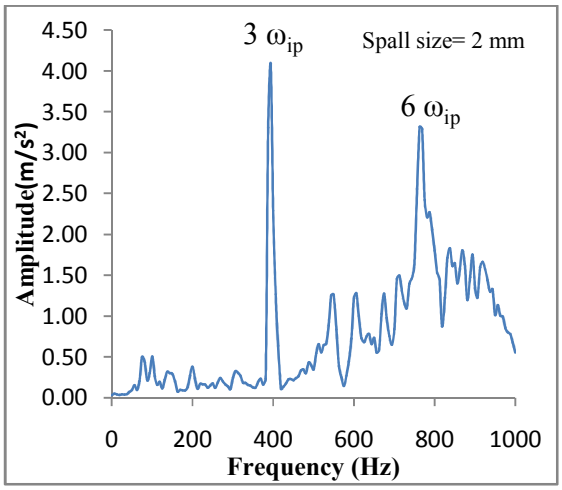

(b) Bearing with spall on inner race

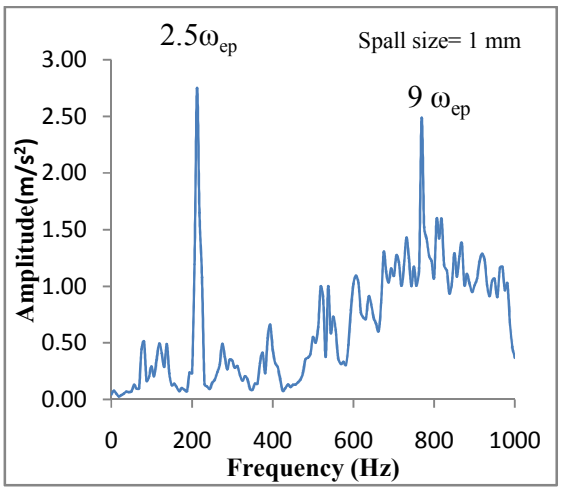

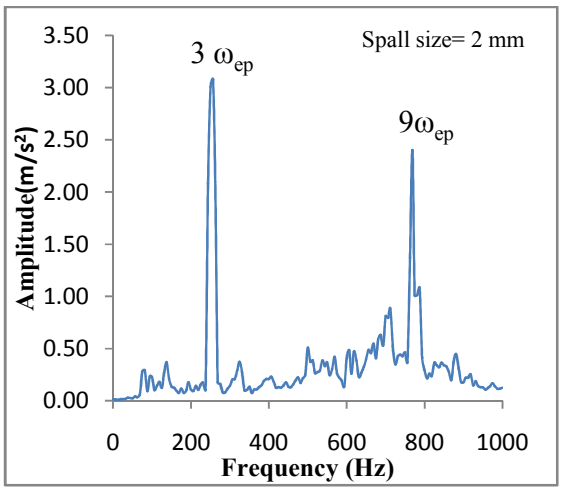

(c) Bearing with spall on outer race

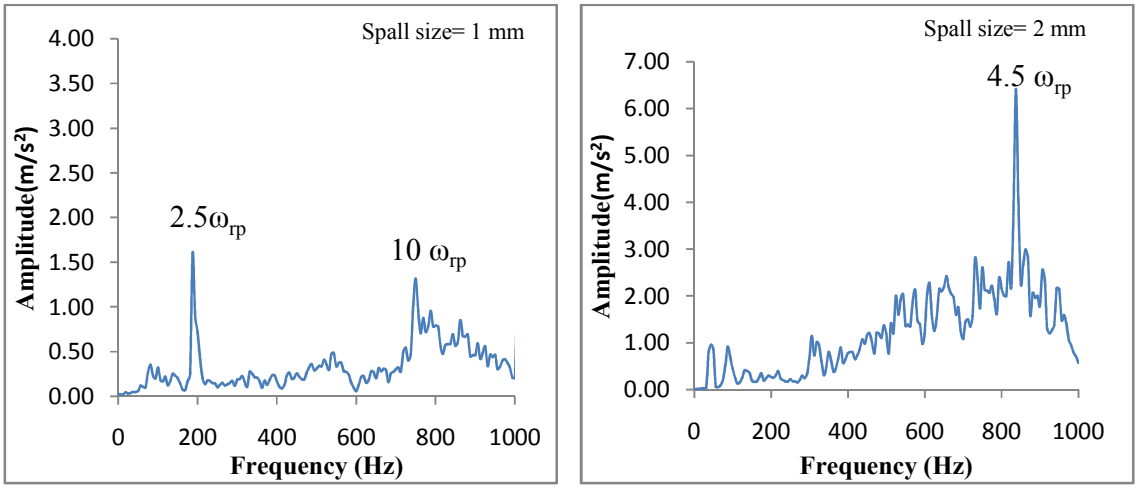

(d) Bearing with spall on roller

Figure 4.44 Vibration signals for various bearing conditions at rotor speed 1000 RPM

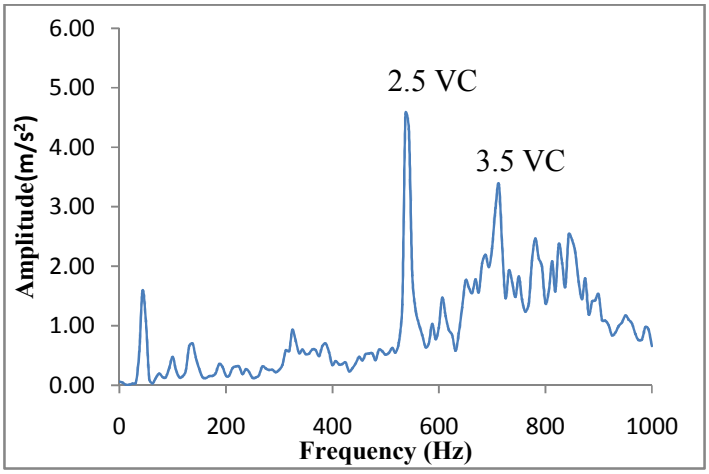

(a) Healthy Bearing

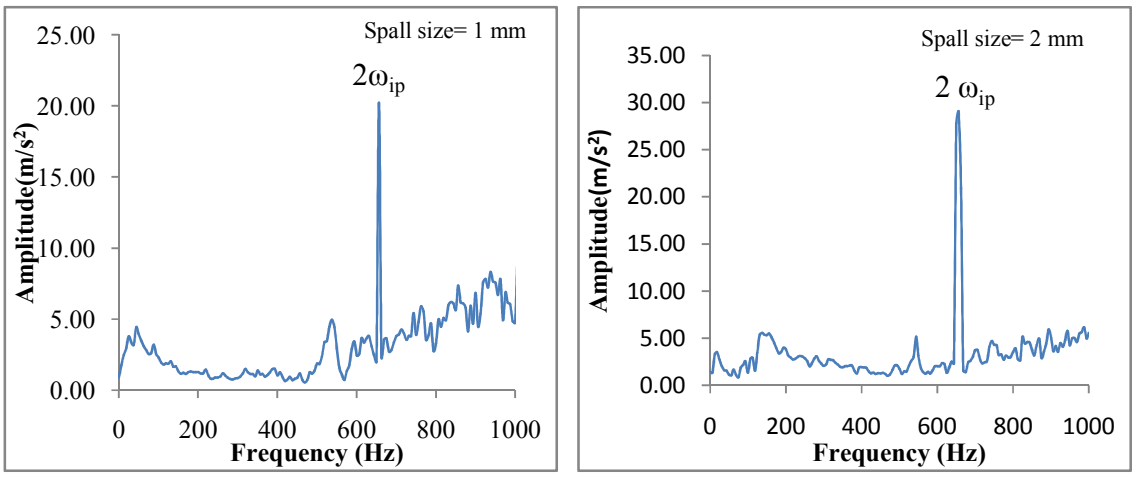

(b) Bearing with spall on inner race

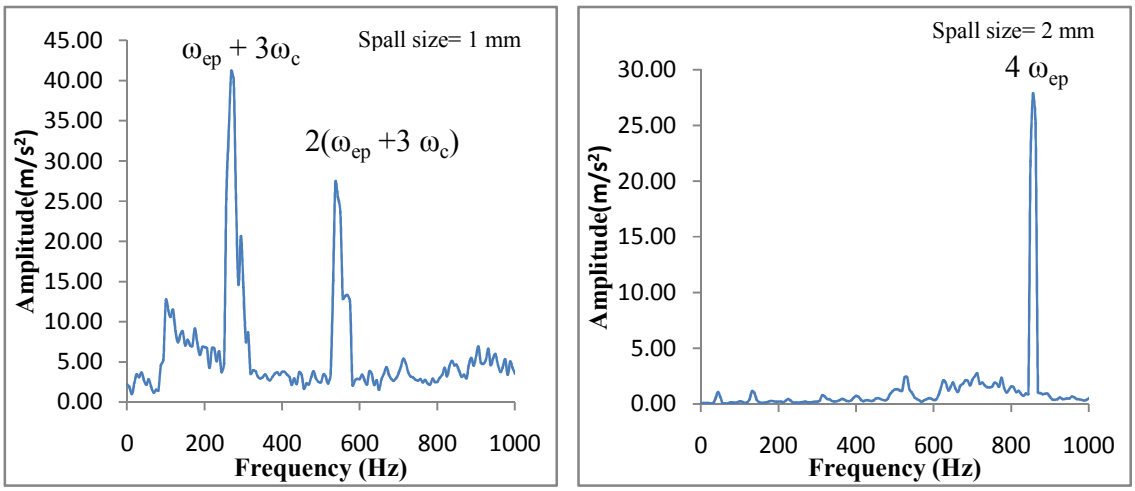

(c) Bearing with spall on outer race

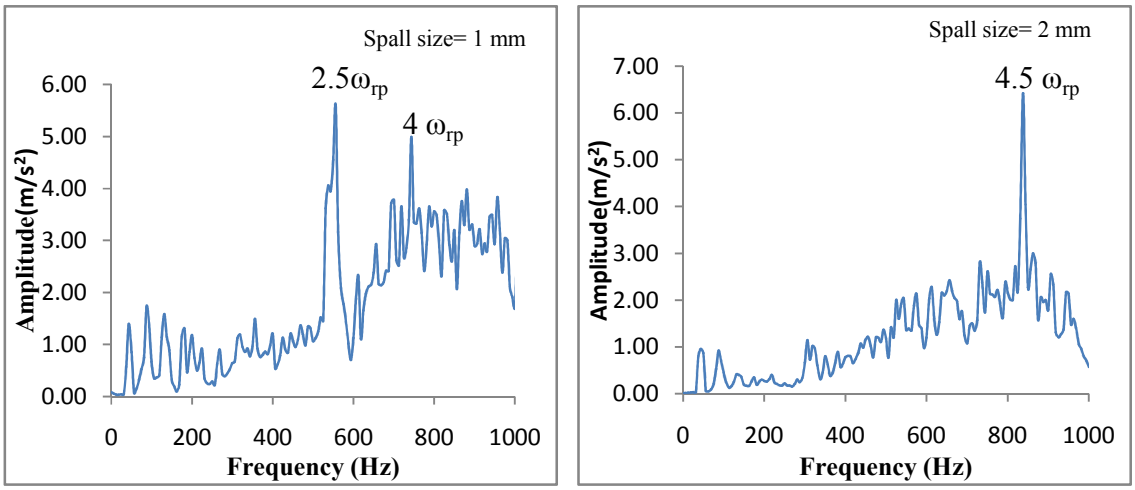

(d) Bearing with spall on roller

Figure 4.45 Vibration signals for various bearing conditions at rotor speed 2500 RPM

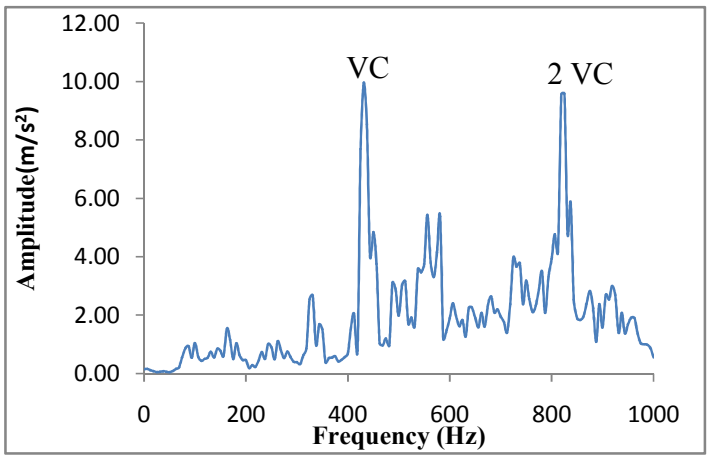

(a) Healthy Bearing

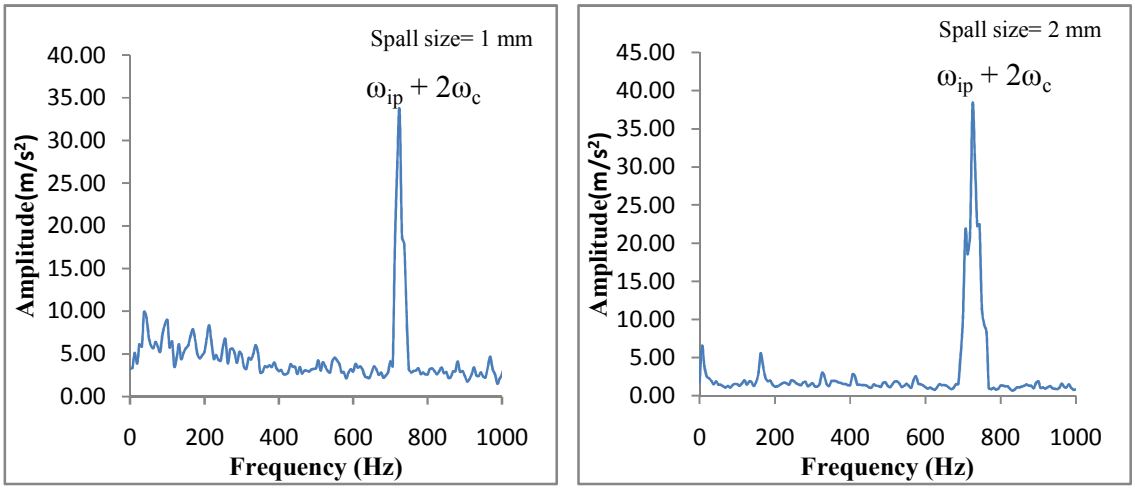

(b) Bearing with spall on inner race

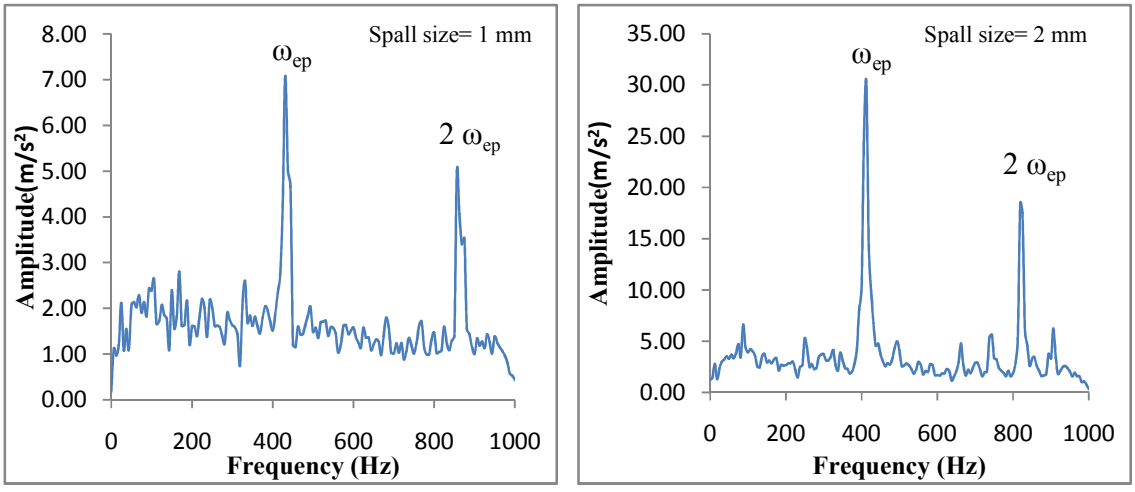

(c) Bearing with spall on outer race

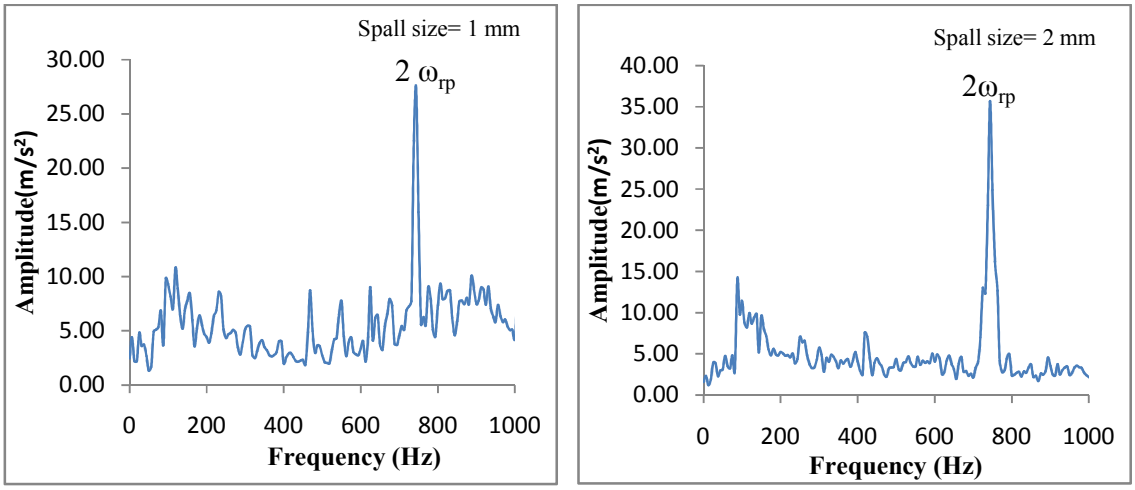

(d) Bearing with spall on roller

Figure 4.46 Vibration signals for various bearing conditions at rotor speed 5000 RPM

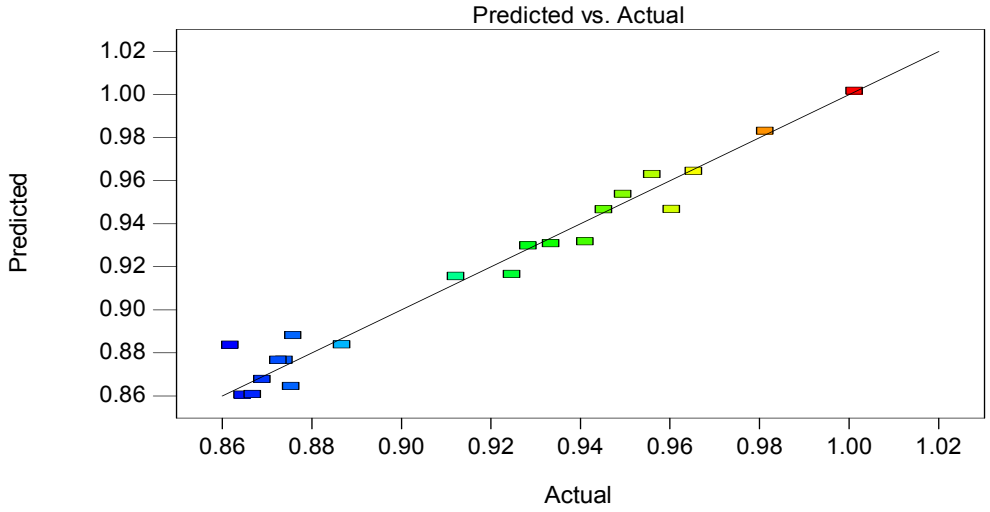

Figure 4.47 The performance prediction of amplitude response

Table 4.10 Analysis of Variance Table for Acceleration [Partial Sum of Squares - Type III]

Source	**Sum of Squares**	**Df**	**Mean Square**	**F Value**	**p-value (Prob > F)**
Model	0.037	12	3.120E-003	19.74	0.0001
A-Inner Race Defect	4.963E-003	1	4.963E-003	31.41	0.0005
B-Outer Race Defect	2.911E-003	1	2.911E-003	18.42	0.0026
C-Roller Defect	1.165E-006	1	1.165E-006	7.375E-003	0.9337
D-Speed	5.878E-004	1	5.878E-004	3.72	0.0899
BD	1.333E-008	1	1.333E-008	8.438E-005	0.9929
CD	1.248E-004	1	1.248E-004	0.79	0.4001
A^2	8.522E-004	1	8.522E-004	5.39	0.0487
B^2	1.144E-004	1	1.144E-004	0.72	0.4195
D^2	1.516E-003	1	1.516E-003	9.60	0.0147
B^2D	1.207E-003	1	1.207E-003	7.64	0.0245
BD^2	4.301E-004	1	4.301E-004	2.72	0.1376
CD^2	9.344E-004	1	9.344E-004	5.91	0.0411
Residual	1.264E-003	8	1.580E-004		
Cor Total	0.039	20			

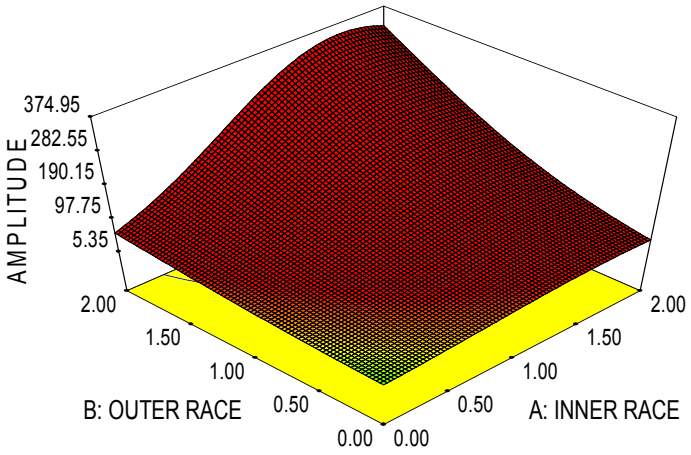

Figure 4.48 Acceleration response surfaces showing interaction of parameter A and B

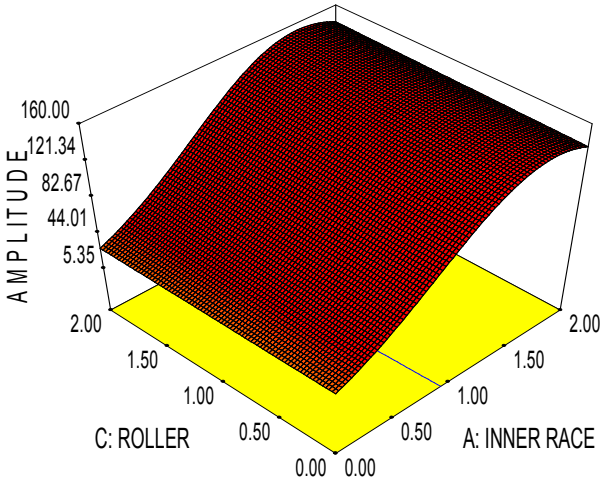

Figure 4.49 Acceleration response surfaces showing interaction of parameter A and C

Response surfaces show the interactive effects of defects on various components with each other. Interaction effects of bearing component defects on each other are as shown in Figure 4.48 and 4.49. Figure 4.48 shows that the amplitude of the vibration gradually increases with inner race defect and outer race defect individually. But when both inner race defect and outer race defect occurs simultaneously, as the defect increases, the amplitude of vibration rapidly increases. Figure 4.49 shows that the roller with spall has less effect on amplitude of vibration. While inner race defect has significant effect on amplitude of vibration, if spall on roller and inner race simultaneously exist.

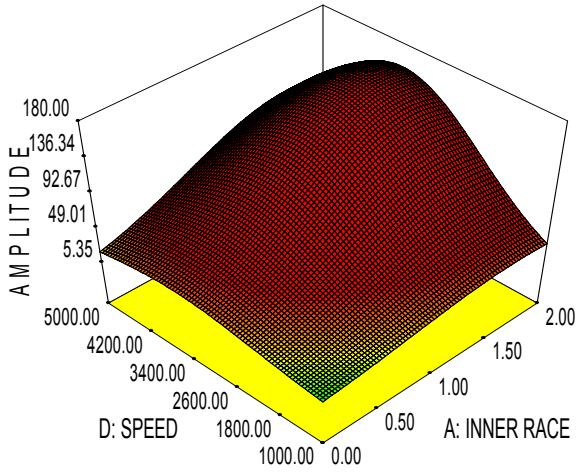

Figure 4.50 Acceleration response surfaces showing interaction of parameter A and D

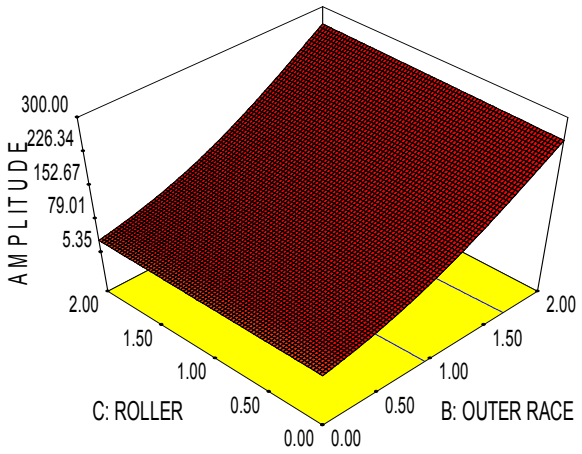

Figure 4.51 Acceleration response surfaces showing interaction of parameter B and C

Response surface in Figure 4.50 shows that interaction effects of speed with inner race defect. This shows that the individual effect of speed and inner race defect variation is not much. But effect of inner race defect with high speed of rotor is more significant on amplitude of vibration. When inner race defect is 2 mm and speed is 5000 rpm, amplitude of vibration is decreased due to '*self peening*' phenomenon which indicates bearing enters in catastrophic stage of failure. Figure 4.51 shows that the roller with spall has less effect on amplitude of

vibration. But amplitude of vibration increased significantly as severity of outer race defect increases.

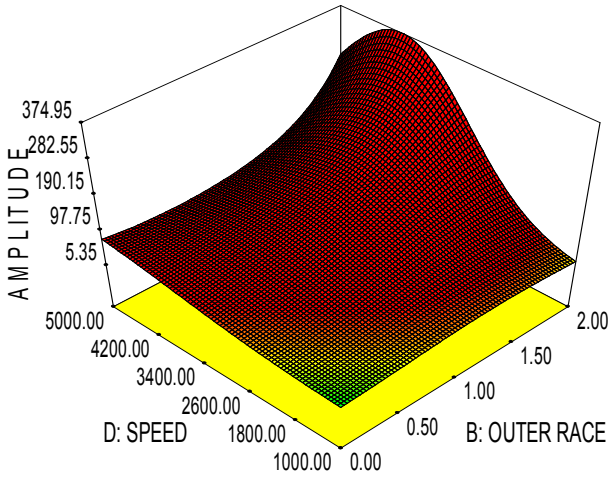

Figure 4.52 Acceleration response surfaces showing interaction of parameter B and D

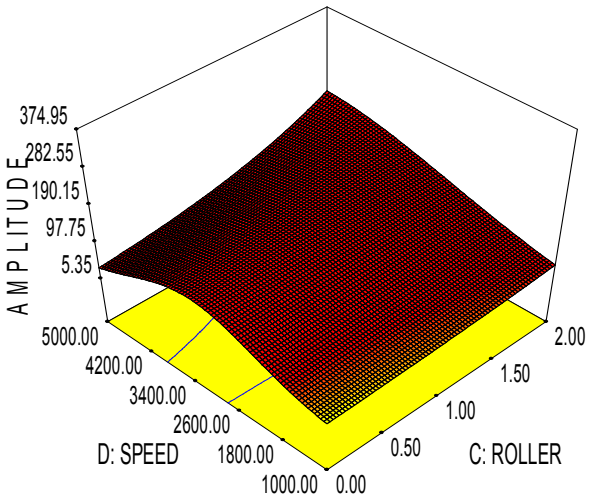

Figure 4.53 Acceleration response surfaces showing interaction of parameter C and D

Figure 4.52 and 4.53 shows the interaction effect of the rotor speed with outer race defect and ball defect respectively and indicate that the speed of rotor has significant effect on

amplitude of vibration. With speed variation, it can be seen that the outer race defect has significant effect on vibration response as compare with roller defect.

From the response surfaces showing interaction between various factors it is concluded that the outer race defect has most significant effect on amplitude of vibration and roller defect has least effect on vibration response. Rotor speed is another important parameter having significant effect on vibration response. At higher speed, presence of spall on outer or inner race may result in catastrophic failure. The flow chart used for analysis using RSM is as shown in Figure 4.54.

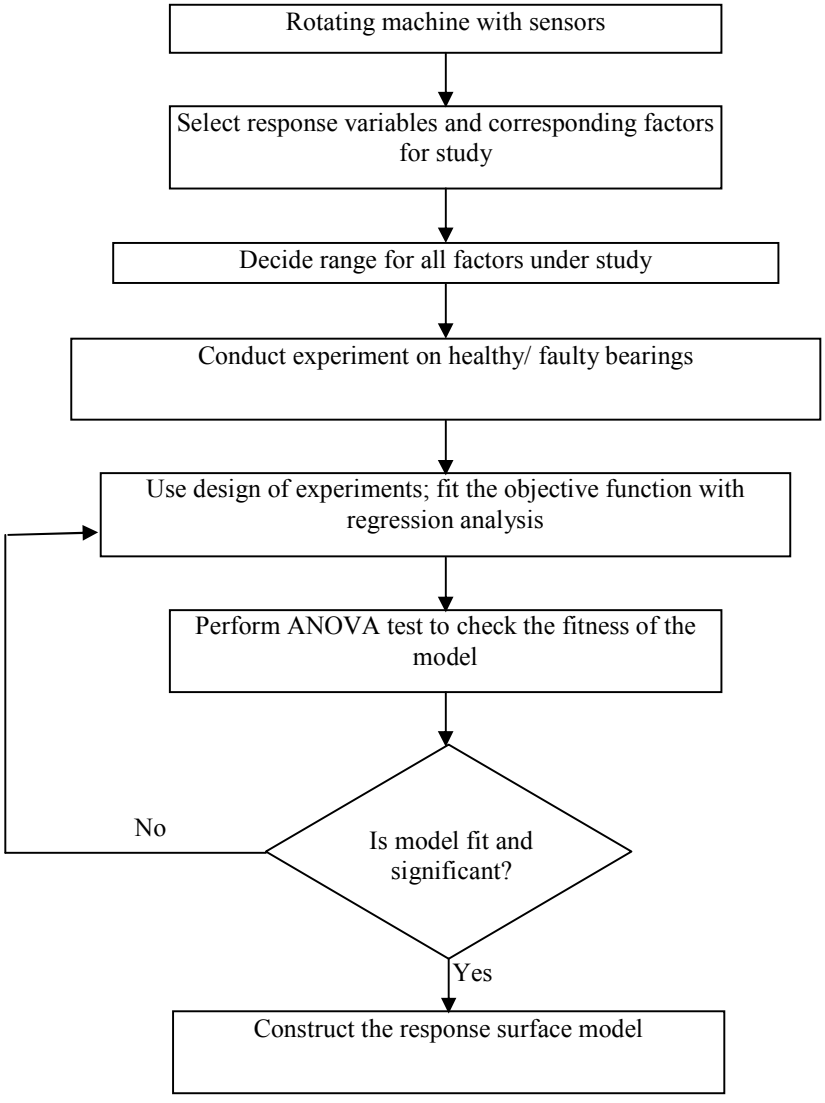

Figure 4.54 The Flow Chart of RSM

CHAPTER 5
CONCLUSIONS

In most of the studies, the fault diagnosis of rolling element bearings has been focused mainly on vibration measurement methods and utilization of these methods for detecting faults on individual components. However, very few studies have been carried out and reported in literature, which address the effect of severity of localized defects of bearing components on the nature of the vibration response. In the present study, localized defect has been considered on the taper roller bearing. The dynamic behaviour of healthy/faulty taper roller bearing elements is investigated. The vibration response due to localized defects on the inner race, outer race and roller have been demonstrated, also combination of these defects and rotational speed. Following important conclusions as regards the effects of localized defect on dynamic response from the present study can be made:

5.1 EFFECTS OF LOCALIZED DEFECTS FOR TAPER ROLLER BEARINGS

In the present investigation, experimental study of a rotor bearing system has been carried out to obtain the vibration response due to localized defects such as spall on outer race, inner race and roller. From the vibration responses of rotor bearing system due to localized defects, the following conclusions may be drawn.

5.1.1 Spall on Outer Race

a) For spall of size 1 mm in the outer race, the peak amplitude in spectrum appears on the multiples of rolling element passage frequency of outer race ($2.5\omega_{ep}$) for the rotor speed upto 2000 rpm.

b) As the speed increases further upto 3500 rpm, peak appears as an interaction of rolling element passage frequency of outer race and cage frequency ($\omega_{ep} + 3\omega_c$). For further increase in speed, the peak appears on the rolling element passage frequency of outer race (ω_{ep}) and its harmonics. This is also concluded by Kankar (2011).

5.1.2 Spall on Inner Race

a) For inner race defect, the peak amplitude appears in the vibration spectrum at the twice of rolling element passage frequency of inner race ($2\omega_{ip}$) upto 2500 rpm. For higher speed,

peak appears as an interaction of rolling element passage frequency of inner race with cage frequency.

b) Other major peaks are appeared at the harmonics of rolling element passage frequency of inner race (ω_{ip}) and its interaction with multiple cage frequency.

5.1.3 Spall on Roller

For roller defect, the spectrum has components at the multiples of the rolling element passage frequency of roller also known as roller spin frequency.

5.2 RESPONSE SURFACE METHOD

In the present experimental investigation, dynamic responses of a healthy/faulty taper roller bearing have been also analyzed and predicted using response surface methodology. DOE and RSM procedures are used to conduct several trials for investigating simultaneous effect of localized defects and rotor speed. These factors are considered with three levels and total 21 trials have been conducted as described in Table 4.9. From the obtained responses, the following conclusions are drawn:

a) Severe vibration (Max. peak of vibration excitation) occurs in case of bearing with outer race defect. Also interaction of outer and inner race defect produces severe vibrations. Defect in roller has less effect on amplitude of vibration.

b) In some cases (Figures 4.50 and 4.52), vibration amplitudes due to interaction of speed with inner race and outer race defect is reduced. This indicates that the catastrophic failure occurs and due to self-peening of the bearing defects, amplitude levels are decreased.

c) Vibration responses due to interaction in outer race defect and roller defect increases.

d) Outer race defect has significant effect on vibration response as compared with inner race defect and roller defect.

REFERENCES

1. Abbasiona, S., Rafsanjania, A., Farshidianfarb, A., Iranic, N., Rolling Element Bearings Multi-fault Classification Based on the Wavelet Denoising and Support Vector Machine, Mechanical Systems and Signal Processing, Vol. 21, 2007, pp. 2933–2945.
2. Arslan, H. and Aktürk, N., An Investigation of Rolling Element Vibrations Caused by Local Defects, ASME Journal of Tribology, Vol. 130, 2008, pp. 041101-12.
3. Bachschmid, N., Pennacchi, P., Vania, A., Identification of Multiple Faults in Rotor Systems, Journal of Sound and Vibration, Vol. 254(2), 2002, pp. 327-366.
4. Brändlein, J., Eschmann, P., Hasbargen, L., Weigand, K., Ball and Roller Bearings-Theory, Design and Application. Third edition, John Wiley & Sons, Ltd. (UK), 1999.
5. Box, G.E.P. and Wilson, K.B., On the experimental attainment of optimum conditions, Journal of Royal. Statistical Society, Series B, Vol. 13 (1), 1951, pp. 1-35.
6. Changqing, B., Qingyu, X., Dynamic Model of Ball Bearings with Internal Clearance and Waviness, Journal of Sound and Vibration, Vol. 294, 2006, pp. 23–48.
7. Changqing, B., Qing-yu, X., Xiao-long Z., Nonlinear Stability of Balanced Rotor Due to Effect of Ball Bearing Internal Clearance, Applied Mathematics and Mechanics, Vol. 27, 2006, pp. 175-186.
8. Chen, P., Bearing Condition Monitoring and Fault Diagnosis. M S Thesis, The University Of Calgary, Calgary, Alberta, 2000.
9. Gallina, A., Martowicz, A., Uhl, T., An Application of Response Surface Methodology in the Field of Dynamic Analysis of Mechanical Structures Considering Uncertain Parameters, ISMA 2006 Conference, Leuven, Belgium.
10. Harris, T.A., Kotzalas, M.N., Essential Concepts of Bearing Technology. CRC Press, Boca Raton, FL, 2006.
11. Harsha, S.P., Kankar, P.K., Stability Analysis of a Rotor Bearing System Due to Surface Waviness and Number of Balls, International Journal of Mechanical Sciences, Vol. 46, 2004, pp. 1057–1081.

12. Harsha, S.P., Non-linear Dynamic Analysis of an Unbalanced Rotor Supported by Rolling Bearing, Chaos, Solitons and Fractals, Vol. 26, 2005(b), pp. 47–66.

13. Harsha, S.P., Nonlinear Dynamic Analysis of Rolling Element Bearings Due to Cage Run-Out and Number of Balls, Journal of Sound and Vibration, Vol. 289, 2006, pp. 360–381.

14. Harsha, S.P., Non-linear Dynamic Response of a Balanced Rotor Supported on Rolling Element Bearings, Mechanical Systems and Signal Processing, Vol. 19, 2005(a), pp. 551–578.

15. Harsha, S.P., Nonlinear Dynamic Response of a Balanced Rotor Supported by Rolling Element Bearings Due to Radial Internal Clearance Effect, Mechanism and Machine Theory, Vol. 41, 2006, pp. 688–706.

16. Harsha, S.P., Kumar, S., Prakash, R., Non-linear Dynamic Behaviors of Rolling Element Bearings Due to Surface Waviness, Journal of Sound and Vibration Vol.272, 2004, pp. 557–580.

17. Jardine, A., Lin D., Banjevic D., A Review on Machinery Diagnostics and Prognostics Implementing Condition-Based Maintenance, Mechanical Systems and Signal Processing, Vol. 20, 2006, pp. 1483-1510.

18. Jun, M., Detection of Localised Defects in Rolling Element Bearings via Composite Hypothesis Test, Mechanical Systems and Signal Processing, Vol. 9(1), 1995, pp 63-75.

19. Kankar, P.K., Harsha, S.P., Kumar, P., Sharma, S.C., Fault Diagnosis of a Rotor Bearing System using Response Surface Method, European Journal of Mechanics A/Solids, Vol. 28, 2009, pp. 841–857.

20. Kankar, P.K., Sharma, S. C., Harsha, S.P., Fault Diagnosis of Ball Bearings using Machine Learning Methods, Expert Systems with Applications, Vol. 38, 2011, pp. 1876–1886 .

21. Kankar, P.K., Sharma, S.C., Harsha, S.P., Fault Diagnosis of Ball Bearings using Continuous Wavelet Transform, Applied Soft Computing, Vol. 11, 2011, pp. 2300–2312.

22. Kankar, P.K., Fault Diagnosis of Rolling Element Bearings Using Vibration Signature Analysis. PhD Thesis, Indian Institute of Technology Roorkee, Roorkee, 2011.

23. Karacay, T., Akturk, N., Experimental Diagnostics of Ball Bearings using Statistical and Spectral Methods, Tribology International, Vol. 42, 2009, pp. 836–843.

24. Kiral, Z., Karagulle, H., Vibration Analysis of Rolling Element Bearings with Various Defects Under the Action of an Unbalanced Force, Mechanical Systems and Signal Processing, Vol. 20, 2006, pp. 1967–1991.

25. Kurfess, T.R., Billington, S., Liang, S.Y., Advanced Diagnostic and Prognostic Techniques for Rolling Element Bearings, Condition Monitoring and Control for Intelligent Manufacturing, 2006, pp. 137-165.

26. Lai, M.S., Developing Bearing Failure by Mean of Vibration Analysis. PhD Thesis, University of Windsor, Ontario, Canada, 1990.

27. Lim, T.C., Singh, R., Vibration Transmission through Rolling Element Bearings Part 1: Bearing Stiffness Formulation, Journal of Sound and Vibration, Vol. 139, 1990, pp. 179-199.

28. Laniado-Jacome, E., Meneses-Alonso, J., Diaz-Lopez, V., A Study of Sliding between Rollers and Races in a Roller Bearing with a Numerical Model for Mechanical Event Simulations, Tribology International, Vol. 43, 2010, pp. 2175–2182.

29. Mori, K., Kasashima, N., Yoshioka, T., Ueno, Y., Prediction of Spalling on a Ball Bearing by Applying the Discrete Wavelet Transform to Vibration Signals, Wear, Vol. 195, 1996, pp. 162-168.

30. Nataraj, C., Harsha, S.P., The Effect of Bearing Cage Run-Out on the Nonlinear Dynamics of a Rotating Shaft, Communications in Nonlinear Science and Numerical Simulation, Vol. 13, 2008, pp. 822–838.

31. Orhan, S., Akturk, N., Celik, V., Vibration Monitoring for Defect Diagnosis of Rolling Element Bearings as a Predictive Maintenance Tool: Comprehensive Case studies, NDT&E International, Vol. 39, 2006, pp. 293–298.

32. Prasad, H., Theoretical and Experimental Investigations on the Pitch and Width of Corrugations on the Surfaces of Ball Bearings, Wear, Vol.143, 1991, pp. 1-14.

33. Patil, M.S., Mathew, J., Rajendrakumar, P.K., Desai, S., A Theoretical Model to Predict the Effect of Localized Defect on Vibrations Associated with Ball Bearing, International Journal of Mechanical Sciences, Vol. 52, 2010, pp. 1193–1201.

34. Purushothama, V., Narayanana, S., Suryanarayana, A.N. Prasad, Multi-Fault Diagnosis of Rolling Bearing Elements using Wavelet Analysis and Hidden Markov Model Based Fault Recognition, NDT & E International, Vol. 38, 2005, pp. 654–664.

35. Rafsanjania, A., Abbasiona, S., Farshidianfarb, A., Moeenfardc, H., Nonlinear Dynamic Modeling of Surface Defects in Rolling Element Bearing Systems, Journal of Sound and Vibration, Vol. 319, 2009, pp. 1150–1174.

36. Rahnejat, H. and Gohar, R., The Vibrations of Radial Ball Bearings, Proceedings of the Institution of Mechanical Engineers, Part C: Journal of Mechanical Engineering Science, Vol. 199(C3), 1985, pp. 181-193.

37. Sawalhi, N., Randall, R.B., Vibration Response of Spalled Rolling Element Bearings: Observations, Simulations and Signal Processing Techniques to Track the Spall Size, Mechanical Systems and Signal Processing, Vol. 25, 2011, pp. 846–870.

38. Silberwolf, B., http://en.wikipedia.org/wiki/Tapered_roller_bearing, 2006.

39. Su, W., Wang, F., Zhu, H., Zhang, Z., Guo, Z., Rolling Element Bearing Faults Diagnosis Based on Optimal Morlet Wavelet Filter and Autocorrelation Enhancement, Mechanical Systems and Signal Processing, Vol.24, 2010, pp.1458–1472.

40. Tandon, N., Choudhury, A., An Analytical Model for the Prediction of the Vibration Response of Rolling Element Bearings Due to a Localized Defect, Journal of Sound and Vibration, Vol. 205(3), 1997, pp. 275-292.

41. Tandon, N., Choudhury, A., A Review of Vibration and Acoustic Measurement Methods for the Detection of Defects in Rolling Element Bearings, Tribology International, Vol. 32, 1999, pp.469–480.

42. Tomovic, R., Miltenovic, V., Banic, M., Miltenovic, A., Vibration Response of Rigid Rotor in Unloaded Rolling Element Bearing, International Journal of Mechanical Sciences, Vol. 52, 2010, pp. 1176–1185.

43. Trendafilova, I., An Automated Procedure for Detection and Identification of Ball Bearing Damage using Multivariate Statistics and Pattern Recognition, Mechanical Systems and Signal Processing, Vol. 24, 2010, pp. 1858–1869.